Computational Fluid Dynamics Investigation on Radon Concentration in Residential Buildings

by

Titu Wilson

Bachelor of Technology, Aeronautical Engineering,

A.P.J Abdul Kalam Technological University, 2020

A Thesis Submitted in Partial Fulfillment of the Requirements for the Degree of

Master of Applied Science

In the Department of Mechanical Engineering

© Titu Wilson, 2025

University of Victoria

All rights reserved. This thesis may not be reproduced in whole or in part, by photocopy or other means, without the permission of the author.

We acknowledge and respect the Lək̓ʷəŋən (Songhees and Xʷsepsəm/Esquimalt) Peoples on whose territory the university stands, and the Lək̓ʷəŋən and W̱SÁNEĆ Peoples whose historical relationships with the land continue to this day.

Computational Fluid Dynamics Investigation on Radon Concentration in Residential Buildings

by

Titu Wilson

Bachelor of Technology, Aeronautical Engineering,

A.P.J Abdul Kalam Technological University, 2020

Supervisory Committee

Dr. Caterina Valeo, Co-supervisor

Department of Mechanical Engineering

Dr. Phalguni Mukhopadhyaya, Co-supervisor

Department of Civil Engineering

Abstract

Radon, a naturally occurring radioactive gas formed from uranium decay, is a significant health hazard and the leading cause of lung cancer among the general population. Radon gas can infiltrate building structures through cracks and openings in the building envelope. The concentration inside the building is influenced by factors such as indoor temperature, humidity, and ventilation rates.

This study focuses on a case study house in Victoria, BC, Canada where radon measurements were taken for over a six-week period during the heating season to capture real-world indoor radon behaviour. A combination of real-world data collection, analytical calculations, and computational fluid dynamics (CFD) simulations were used to analyze radon concentration patterns under varying temperature, humidity, and ventilation conditions. The CFD model was developed using ANSYS Fluent, with the indoor environment simulated under different temperatures (18°C, 21°C, and 24°C) and humidity (20%, 40%, and 60%) conditions at an air change rate of 0.5 ACH (air change per hour) from the field experiment.

Numerical and experimental (field) observations revealed that indoor temperature significantly influences radon concentration, with higher temperatures enhancing the stack effect, leading to increased radon levels. Numerical simulations showed that humidity also played a critical role, where higher humidity levels acted as a barrier to radon infiltration, reducing its accumulation. The study validated the CFD model by comparing it with measured field data and analytical results, demonstrating less than a 2% difference, confirming its reliability.

This research contributes valuable insights into indoor radon concentration and behaviour, emphasizing the importance of maintaining optimal indoor environmental conditions to manage radon exposure. The findings highlight the need for integrated radon mitigation strategies, considering temperature, humidity, and ventilation to ensure safer indoor air quality in residential buildings in Victoria, BC, Canada. These insights can inform building design, public health policies, and radon management practices, helping to reduce radon-related health risks.

Table of Contents

List of Figures

List of Tables

Abbreviations

Abbreviation	Definition
^{222}Rn	Radon-222
^{238}U	Uranium-238
^{234}Th	Thorium-234
^{226}Ra	Radium-226
^{218}Po	Polonium-218
keV	Kilo-electron Volt
WHO	World Health Organization
EPA	Environmental Protection Agency
IAQ	Indoor Air Quality
ASD	Active Soil Depressurization
Bq/m^3	Becquerels per Cubic Meter
ACH	Air Change Rate per Hour
CFD	Computational Fluid Dynamics
ASHRAE	American Society of Heating, Refrigerating and Air-Conditioning Engineers
CAN/CSA	Canadian Standards Association
NBC	National Building Code
EICs	Electret Ion Chambers
FVM	Finite Volume Method
FDM	Finite Difference Method
FEM	Finite Element Method
PDE	Partial Differential Equation
SST	Shear Stress Transport
Cp	Specific Heat Capacity
MW	Molecular Weight
SI	International System of Units
ALARA	As Low as Reasonably Achievable
HVAC	Heating, Ventilation, and Air Conditioning

Notations

A	Exhalation surface area (m^2)
ACH	Air change rate (h^{-1})
C	Radon concentration (Bq/m^3)
C_0	Initial radon concentration (Bq/m^3)
Cp	Specific heat capacity (J/kg K)
D	Diffusion coefficient (m^2/s)
E	Radon exhalation rate ($Bq/m^2 \cdot h$)
g	Gravitational acceleration (m/s^2)
h	Specific enthalpy (J/kg)
K	Thermal conductivity (W/m K)
MW	Molecular weight (kg/k_{mol})
p	Pressure (Pa)
RH	Relative humidity (%)
S	Radon generation rate ($Bq/m^3 \cdot s$)
T	Temperature (°C or K)
V	Velocity vector (m/s)
V	Volume of the room (m^3)

Greek Symbols

v	Inlet velocity (m/s)
λ	Total decay rate (s^{-1})
λRn	Radon decay constant (s^{-1})
λv	Ventilation rate constant (s^{-1})
μ	Dynamic viscosity ($kg/m \cdot s$)
ρ	Density (kg/m^3)
Φ	Dissipation function (W/m^3)

Acknowledgment

I would like to express my sincere gratitude to my research supervisor, Dr. Phalguni Mukhopadhyaya, for his unwavering support, guidance, and insight throughout this research journey. His expertise and willingness to assist at every stage have been invaluable, and I am sincerely grateful for the countless opportunities he provided for my professional growth. His mentorship has not only contributed significantly to the completion of this work but also helped shape my academic and career path.

My sincere thanks also go to my co-supervisor, Dr. Caterina Valeo, for her guidance, encouragement, and constructive feedback. Her support throughout my master's program has been a source of inspiration, and her dedication to my success has been greatly appreciated.

Special thanks to the experts at Radonova and Radonwest for their valuable information, which greatly contributed to the foundation of this study.

I am deeply grateful to Dr. Armando Tura for graciously allowing me to use his house as the case study for this research. His support was instrumental in advancing this project. Additionally, I would like to extend my heartfelt appreciation to Mr. Bastien Lanusse and Ms. Arielle Garrett for their tremendous assistance and dedication in the Building Science Laboratory, which were essential in conducting experiments and collecting data.

Finally, I am thankful to my family, friends, and colleagues who have supported me throughout this journey. Their encouragement and belief in my abilities have motivated me to persevere and complete this research.

Chapter 1 Introduction

Radon (^{222}Rn) is a naturally occurring radioactive noble gas formed from the disintegration of uranium (^{238}U), commonly found in soil, rock, and water [1]. In recent decades, there has been growing attention to the health risks associated with radon exposure, particularly in residential buildings and enclosed structures in contact with the soil. The World Health Organization recognized radon as one of the major contributors to background radiation, accounting for approximately 50% of an individual's total radiation exposure over their lifetime [2]. Prolonged exposure to elevated radon concentrations significantly increases the risk of lung cancer and the risk depends on the concentration and the duration, a person is exposed to the gas [3]. This places radon as a critical factor in indoor air quality assessments, highlighting the importance of understanding and mitigating radon concentrations in residential and commercial buildings.

Uranium is found ubiquitously in the Earth's crust. It undergoes a series of radioactive decay processes forming various intermediate radioactive elements, including thorium-234 (^{234}Th), radium-226 (^{226}Ra), and then radon-222 (^{222}Rn), before stabilizing as lead-206 (^{206}Pb). Among the 37 radioactive isotopes (^{193}Rn to ^{229}Rn), radon-222 (^{222}Rn) is one of the most significant isotopes due to its noble gas status. Unlike many other radioactive decay products, radon-222 can migrate through soil and rocks until it reaches the surface, entering homes and buildings through cracks and joints in foundations, walls, floors, and other openings [4]. Its noble gas state, coupled with its relatively short half-life of 3.82 days, allows radon to accumulate in indoor environments, especially in tightly sealed or poorly ventilated spaces [5].

As radon gas decays into other radioactive particles, such as polonium-218 (^{218}Po), it emits high-energy alpha and gamma radiation [6]; specifically:

1. Alpha emission at 5489.7 keV with an intensity of 99.92%
2. Alpha emission at 4987 keV with an intensity of 0.08%
3. Alpha emission at 4827 keV with an intensity of 0.0005%
4. Gamma emission at 510 keV with an intensity of 0.07%

These alpha particles emitted during the radioactive decay of radon, can attach to dust and aerosols present in the air, when these contaminated particles are inhaled, they become attached to the respiratory system [7]. Once inside the lungs, the alpha particles continue to emit radiation, directly exposing the surrounding lung tissues to ionizing radiation. This exposure can damage cellular structures and DNA, potentially leading to mutations. Over the time, such damage may accumulate, increasing the risk of lung cancer [8-9].

Radon exposure is recognized as the leading cause of lung cancer among non-smokers, accounting for approximately 16% of all lung cancer cases worldwide. In Canada alone, radon exposure accounts for more than 3,000 lung cancer deaths annually [10]. Among smokers, radon exposure further exacerbates cancer risk, making it the second leading cause of lung cancer. The combination of smoking and radon exposure creates a synergistic effect, significantly increasing the overall risk of developing lung cancer.

The growing awareness of radon's health implications began in the 1980s, as reports of respiratory illnesses linked to elevated indoor radon levels surfaced [11]. This realization prompted National authorities to regulate and manage radon exposure, resulting in building codes and standards that are now incorporate radon-resistant construction techniques. Common mitigation measures now include the installation of radon barriers, vapor membranes, active soil depressurization (ASD) systems, radon rough-ins, and sealing foundation cracks to prevent radon entry from the ground [12-13]. However, despite these efforts, indoor radon concentrations can still be influenced by other environmental factors such as indoor temperature, humidity, ventilation rates, and pressure differentials between indoor and outdoor spaces [14]. As buildings become more airtight to enhance energy efficiency, the potential for radon accumulation increases, making it essential to consider the environmental factors for effective radon management strategies.

Global health organizations have established guidelines to limit indoor radon concentrations. The World Health Organization (WHO) recommends that radon levels not exceed 100 Bq/m^3 and Health Canada set a threshold of 200 Bq/m^3 [15]. Adhering to these guidelines requires regular radon testing and implementing mitigation strategies to manage and maintain safe indoor radon levels.

Computational Fluid Dynamics (CFD) is one of the most promising tools for studying radon behavior and distribution in indoor environments [16]. CFD simulations provide a cost-effective

and flexible approach to understanding radon distribution by allowing researchers to model complex interactions between radon gas and various environmental factors. Unlike traditional experimental methods, which can be costly and time-consuming, CFD offers the ability to investigate different scenarios and conditions in a controlled, virtual environment. This makes it possible to assess how temperature, humidity, ventilation rates, and building design changes can influence radon levels in different indoor settings [17].

Several studies have employed Computational Fluid Dynamics (CFD) to analyze radon concentrations and distribution patterns. For instance, Akbari et al. (2013) used a CFD model to investigate radon behavior in a single-family detached home in Stockholm, focusing on how heat recovery ventilation systems affect radon levels entering from the floor [18]. Similarly, Chauhan et al. (2014) studied radon distribution using CFD in a closed test room, in India, demonstrating that radon flux from building materials and the room's ventilation rate plays a crucial role in radon dispersion [19]. Moreover, Adelikhah et al. (2023) and Rabi & Oufni (2017) highlighted the importance of airflow velocity and ventilation strategies in managing radon concentrations effectively in Morrocco [20-21]. However, despite Canada’s large uranium deposits and higher potential for residential radon, there are only a few studies from Canadian contexts. While radon surveys have been conducted across Canada(Chen et al., 2012; Khan et al., 2021; Stanley et al., 2017; Whyte et al., 2019), there is an absence of numerical simulation-based research on radon concentration behavior in Canadian houses [22-26]. This study addresses the gap by combining numerical simulations and field experiments for the first time to examine radon dynamics in residential buildings in Victoria, British Columbia, Canada.

1.1 Research Objective

The primary objective of this research is to explore radon concentration in a Canadian residential home using experimental monitoring and CFD modeling. The study aims to conduct indoor radon measurements within a residential setting over an extended period and to develop a CFD model for radon dispersion utilizing ANSYS Fluent to simulate radon behavior in an indoor environment.

1.2 Significance of the Study

The significance of this research is multifaceted, with implications for public health, building design, and radon mitigation strategies**.** Understanding how environmental factors such as

temperature, humidity, and ventilation influence radon levels is crucial for protecting the health of building occupants. Given the significant health risks associated with radon exposure, the findings from this study can contribute to reducing lung cancer incidence rates by informing better radon management practices. Insights from this research can guide architects, engineers, and builders in designing and constructing buildings that minimize radon infiltration and accumulation, especially in areas known to have high radon potential. This study can contribute to developing building codes and standards that incorporate radon-resistant features. This knowledge can help homeowners, building managers, and policymakers implement more efficient radon mitigation strategies, ensuring safer living environments.

1.3 Thesis Structure

The thesis is organized into the following chapters to provide a comprehensive exploration of the study:

- Chapter 1: Introduction – Establishes the background, problem statement, research objectives, significance, and structure of the thesis.
- Chapter 2: Background and Literature Review – Offers an in-depth examination of radon's characteristics, health impacts, indoor distribution patterns, mitigation strategies, and the role of CFD in studying radon behavior.
- Chapter 3: Methodology – Details the research design, including the setup of CFD simulations, material properties, boundary conditions, and the specific scenarios analyzed. It explains how different temperature, humidity, and ventilation conditions are incorporated into the simulation model.
- Chapter 4: Results and Observations – Presents the outcomes of the CFD simulations, showcasing how indoor environmental factors influence radon distribution and concentration. This chapter includes detailed analysis and visualization of radon behavior under different conditions and interprets the results, linking them to the research objectives and questions.
- Chapter 5: Conclusions and Recommendations – This chapter summarizes how environmental factors interact to influence radon behavior and outlines the future scope of the study in advancing radon mitigation research and its practical applications.

Chapter 2 Background and Literature Review

This chapter provides a comprehensive overview of previous research on the influence of environmental factors on radon concentration, transport mechanisms, and radon behavior. It also covers ventilation strategies, radon modeling techniques, detection methods, and the use of Computational Fluid Dynamics (CFD) in studying radon distribution and mitigation.

2.1 Factors Affecting Radon Concentration

A study revealed that Canadians spend over 90% of their lives indoors, at home, at work, or in transit therefore, Indoor air quality (IAQ) has a large impact on human health [27]. Radon (^{222}Rn) can accumulate in enclosed environments that are in contact with the soil. The rate at which radon is released depends on factors such as soil type, geology, atmospheric conditions (e.g., pressure, wind, humidity), and tectonic faults. Granite-rich soils, active seismic zones, volcanic areas, and geothermal fields are notable sources of radon due to their higher uranium content [28].

The radon concentration is typically low in outdoor environments but can be much higher indoors, ranging from a few dozen to several thousand Bq/m^3 [29]. This significant increase in indoors occurs due to the limited ventilation in enclosed spaces, which traps radon and allows it to accumulate over time.

2.1.1 Radon Transportation and Generation Equation

Radon transport from the soil to indoor environments is influenced by both physical and meteorological factors. Radon atoms can escape through larger air-filled pores in the soil and building materials, eventually reaching the building-air interface, where they can enter indoor air through airflow [30]. The primary mechanisms of radon transport are molecular diffusion and pressure-induced flow, also known as advection.

Diffusion is the process by which radon moves from areas of higher concentration to areas of lower concentration. In this context, radon gas diffuses from the soil or building materials to the indoor

air. The rate of diffusion depends on factors such as the radium content, porosity, moisture, permeability, and structure of the soil [31].

Advection involves the movement of radon due to pressure differences across a building's substructure. The basic mechanism for the entry of this gas into houses is always the pressure difference between the inside and the outside—the pressure inside is a few pascals lower than outside the building [32]. This pressure difference can be caused by various factors, including the stack effect, the vacuum effect (from exhaust fans), and the downwind effect (from wind around a building). The stack effect occurs when indoor temperatures are higher than outdoor temperatures, creating a rising air current that can draw radon from the soil into the building.

The general form of radon transport equation is represented by the advection-diffusion equation describing the transport and change of a substance (C) over time, considering the convection, diffusion, a source term (S), and a decay term (λC).

The equation can be represented as,

$$\frac{\partial C}{\partial t} + \nabla(VC) = \nabla(D\nabla C) + S - \lambda C \qquad eq\ 2.1$$

where, $\partial C/\partial t$ represents the rate of change of the concentration (**C**) (Bq/m^3) with respect to time (t). $\nabla(VC)$ represents the convective transport of the substance, where **V** is the velocity field and ∇ is the gradient operator and $\nabla(D\nabla C)$ represents the diffusive transport of the substance, where **D** is the diffusion coefficient (m^2/s) and **S** represents a source term, which can be a production or addition of the substance. λC represents a decay term, which can be a loss or removal of the substance, where λ is the Radon decay constant ($2.1\times10^{-6}s^{-1}$)

This equation describes how a substance changes in space and time due to the combined effects of convection (movement with the flow), diffusion (movement due to concentration gradients), a source term, and a decay term.

2.1.2 Species Transport Equations in Ansys Fluent

When solving for radon dispersion, ANSYS Fluent applies the species transport equation, which considers convection, diffusion, and source terms. When solving the equations for chemical species, ANSYS FLUENT uses the local mass fraction of each species, Y_i, for the i^{th} species.

(Ansys Fluent 12.0 theory guide - 7.1.1 species transport equations). This conservation equation takes the following general form:

$$\frac{\partial}{\partial t}(\rho Y_i) + \nabla.(\rho \vec{v} Y_i) = \nabla \vec{J}_i + S_i - \lambda C \qquad \textit{eq 2.2}$$

where, $\boldsymbol{\rho}$ is the density of the chemical species or the mixture (kg/m), $\boldsymbol{Y_i}$ is the Mass fraction of species (radon), $\vec{\boldsymbol{v}}$ is the velocity vector (m/s), $\vec{\boldsymbol{J_i}}$ is the diffusion flux of species due to the concentration gradient, $\boldsymbol{S_i}$ is the source term (radon exhalation from surfaces), and $\boldsymbol{\lambda C}$ is the Radon decay constant, which is $2.1\times10^{-6}s^{-1}$.

In laminar flow, the diffusion flux $\vec{J}_i$ can be written as,

$$\vec{J}_i = -\rho D_{i,m} \nabla Y_i - D_T \frac{\nabla T}{T} \qquad \textit{eq 2.3}$$

Ansys Fluent uses Fick's law[1] to model mass diffusion due to concentration gradients, under which the diffusion flux is where $\boldsymbol{D_{i,m}}$ is the mass diffusion coefficient for species $\boldsymbol{i}$. The second

[1] Fick's law describes how a substance (like radon gas) moves from an area of high concentration to a low concentration due to diffusion. $\vec{J}_i = -D\frac{dC}{dx}$ Where C is the concentration of the species (e.g., radon, Bq/m³) and x is the distance in the direction of diffusion (m).

term($-\boldsymbol{D_T}\frac{\boldsymbol{\nabla T}}{\boldsymbol{T}}$) represents thermal diffusion, which is usually small for radon but can become significant with large temperature gradients.

For turbulent diffusion, Ansys Fluent includes the turbulent Schmidt number (S_{ct}):

$$\vec{J}_i = -\left(\rho D_{i,m} + \frac{\mu_t}{S_{ct}}\right)\nabla Y_i - D_T\frac{\nabla T}{T} \qquad eq\ 2.4$$

where $\boldsymbol{\mu t}$ is the turbulent viscosity (kg/m·s), $\boldsymbol{S_{ct}}$ is Schmidt number is typically 0.7 and D_T is the thermal diffusion coefficient. This equation is applied in Ansys Fluent, where species diffuse due to temperature gradient.

To determine the radon concentration in an indoor environment at a given temperature and humidity, Air density $\boldsymbol{\rho}$ is temperature-dependent and can be expressed as

$$\rho = \frac{P}{\mathrm{R}\,.\,T} \qquad eq\ 2.5$$

where $\boldsymbol{P}$ is the atmospheric pressure, $\boldsymbol{R}$ is the specific gas constant, and $\boldsymbol{T}$ is the temperature of the mixture air. Furthermore, the radon diffusion coefficient is influenced by relative humidity (RH), as first reported by Kotrappa et al. (1976). The humidity represents the amount of water vapor present in the air,.. its impact on radon transport must be considered. The relative humidity is defined as:

$$RH = \frac{\mathrm{P_{actual}}}{P_{water}} \times 100\% \qquad eq\ 2.6$$

where $\mathbf{P_{actual}}$ is the actual partial vapor pressure of water, and $\mathbf{P_{water}}$ is the water is the saturation vapor pressure of water. The total pressure can be represented by

$$P = P_{dry\,air} + P_{\,water} \qquad eq\ 2.7$$

This equation indicates that relative humidity influences indoor radon concentration by altering the total pressure field. Changes in humidity affect the diffusion coefficient, leading to variations in radon accumulation and transport. When predicting radon concentration in indoor environments,

both temperature and relative humidity must be accounted for to accurately estimate diffusion and advection mechanisms, which are important in CFD simulations of indoor radon transport.

2.1.3 The Role of Ventilation in Indoor Radon Mitigation

Ventilation is critical in maintaining indoor air quality and managing radon levels. Adequate ventilation facilitates the dilution, removal, and replacement of indoor pollutants with fresh air, and helps to reduce radon concentration. According to the American Society of Heating, Refrigerating, and Air-Conditioning Engineers (ASHRAE) Standard 62.1, maintaining acceptable indoor air quality (IAQ) requires adequate ventilation rates [35]. Canadian standards, such as (CAN/CSA 2014; NBC 2010), [36-37] recommend ventilation rates of approximately 5-10 L/s of outdoor air per occupant to maintain healthy indoor conditions (ASHRAE 2016a, 2016b; Health Canada, 2018) [38].

There are two types of ventilation systems exist:

- **Natural Ventilation:** Utilizes pressure differences between indoor and outdoor environments to facilitate airflow through openings in the building envelope.
- **Mechanical Ventilation:** Employs devices like fans, ducts, exhaust systems, and heat recovery ventilation units to force air exchange.

Increasing outdoor air ventilation rates has proven to be one of the most effective ways to dilute indoor radon levels. Studies have shown that when ventilation rates are increased, radon concentrations can be reduced to levels comparable to outdoor air, typically within hours (ASHRAE, 2001) [39]. However, since the 1970s, efforts to improve energy efficiency have led to more airtight buildings with reduced ventilation rates, inadvertently increasing the risk of radon accumulation [40].

2.1.4 Impact of Temperature, Humidity, and Pressure on Radon Infiltration

Indoor air temperature significantly affects radon infiltration through the stack effect, which occurs when warmer indoor air rises and escapes through the building's upper openings, creating a low-

pressure area at the base. This pressure difference draws radon gas into the building through cracks and gaps in the foundation, especially during colder months when indoor heating is prevalent [41].

Humidity and pressure also play crucial roles in radon dynamics. High humidity levels can influence radon transport, as moisture in the air affects diffusion rates. Similarly, changes in indoor air pressure, influenced by wind, temperature differences, and mechanical ventilation, can alter the rate at which radon enters and accumulates indoors. These interactions highlight the importance of understanding how environmental factors influence radon behavior, especially in energy-efficient, airtight buildings.

2.2 Radon Detection Methods and Canadian Guidelines

The Canadian guideline for radon levels in indoor air for dwellings is 200 Bq/m³, which was established by the Federal Provincial Territorial Radiation Protection Committee and adopted by the Government of Canada on June 9, 2007 [42]. Health Canada recommends the building owners to take action within two years if radon levels are between 200 and 600 Bq/m³, and within one year if levels exceed 600 Bq/m³. Long-term radon measurements, lasting from 3 to 12 months, are recommended as radon levels can vary significantly over time. Short-term measurements are not considered adequate for determining the need for remedial action.

Radon levels are reported in Bq/m³ according to the International System of Units (SI) [43]. Health Canada advises homeowners to test their homes using at least one long-term detector for a minimum of 3 months, preferably during the heating season (October to April). Testing should be conducted in a single location, ideally in rooms on the lowest level of the home where occupants spend at least 4 hours per day.

If long-term measurement results are below 200 Bq/m³, further testing is not necessary. While the health risk from radon exposure below this level is considered small, there is still no completely safe level of radon. Homeowners should aim to reduce radon levels as low as reasonably achievable (ALARA). If results exceed 200 Bq/m³, remedial actions are recommended according to the recommended timeframes.

Radon detection devices are categorized into long-term and short-term detectors, according to different monitoring needs. **Long-term detectors**, such as alpha track detectors and electret ion chambers, measure radon levels over periods ranging from 90 days to a year, providing a more accurate average by accounting for seasonal and daily fluctuations. Alpha track detectors use plastic films that capture alpha particle tracks for later microscopic analysis, while electret ion chambers detect voltage drops caused by ionized air from radon decay. **Short-term detectors**, are used for 2 to 7 days, which include activated charcoal adsorption and charcoal liquid scintillation methods, both of which collect radon on charcoal for lab analysis—either through gamma spectroscopy or scintillation techniques. **Continuous radon monitors (CRMs)**, are type electronic devices that use the provide real-time, hourly readings and are often used by professionals for rapid assessments. Choosing the right radon detector depends on the purpose, duration of testing, and building conditions. While long-term detectors offer a comprehensive assessment of radon exposure, short-term detectors and CRMs are useful for quick evaluations.

2.3 Numerical Modeling of Radon Using CFD

Computational Fluid Dynamics (CFD) has emerged as a highly effective tool for simulating and analyzing fluid behavior in complex systems, including indoor airflow. As an advanced computational technique, CFD is widely used to solve mathematical problems related to fluid dynamics by employing numerical methods and algorithms to analyze how fluids behave under various conditions [44].

Computational Fluid Dynamics (CFD) technique can be used for analyzing radon transport and dispersion by solving partial differential equations governing mass, momentum, energy, and species concentration using discretization methods such as the Finite Volume Method (FVM), Finite Difference Method (FDM), and Finite Element Method (FEM). The Finite Volume Method (FVM) is a numerical technique commonly employed in Computational Fluid Dynamics (CFD) software like ANSYS Fluent due to its flexibility and robustness in handling complex geometries and solving fluid flow and heat transfer problems.

To effectively simulate fluid flow and the behavior of radon in indoor environments, the governing equations representing conservation principles of mass, momentum, energy, and species transport

are essential. These equations, typically in the form of Partial Differential Equations (PDEs), capture the complex interactions of radon transport, indoor air conditions, and environmental factors influencing radon concentration and distribution.

2.4 Numerical Solution Approach

Computational Fluid Dynamics software, such as ANSYS Fluent is commonly used to solve these governing equations by transforming the continuous PDEs into discrete algebraic equations using discretization methods. Among these methods, the Finite Volume Method (FVM) is adopted by ANSYS due to its compatibility with unstructured grids and its conservative approach in calculating fluxes across control volume boundaries [45] (Kenway et al., 2019). FVM divides the computational domain into a finite number of small control volumes, integrating the governing equations over each volume to convert them into algebraic forms. According to the ANSYS R2 (2024) manual, the CFD solution process involves steps including creating and meshing the geometry, discretizing the governing equations using the Finite Volume Method, solving them iteratively (e.g., with the SIMPLE algorithm), and post-processing the results [46].

2.5 Current Numerical Simulation Research

Radon concentration modeling in residential buildings has been the subject of extensive research due to its significant health implications. Various studies have employed Computational Fluid Dynamics (CFD) and experimental approaches in residential buildings to understand radon distribution under different environmental and structural conditions.

One of the early studies was conducted by Chauhan et al. (2014), who examined radon distribution in a closed test room (3.01 m × 3.01 m × 3.0 m) using a combination of CFD simulations and experimental validation. Their analysis focused on room characteristics such as wall, floor, and ceiling construction, as well as ventilation rates. The room had three closed doors (0.9 m × 1.99 m) with a door-floor gap of 0.9 m × 0.02 m. For simulation purposes, the door facing the external environment was modeled as the inlet, while the other two served as outlets. The radon exhalation from room surfaces (walls, floor, and ceiling) was considered the only source term.

To determine the surface exhalation rate of radon, an experimental setup was employed using an accumulator and a Scintillation Radon Monitor (SRM). Radon gas was collected via an external pump (1 L/min), and the accumulated radon was measured hourly using SRM. This measurement was a key input for the CFD simulations.

Active monitoring of indoor radon concentration was also conducted using the SRM, which detects alpha particles emitted by radon and its decay products. Passive (time-integrated) measurements were conducted using a single-entry pinhole-based twin cup dosimeter consisting of two chambers with LR-115 films. Fifteen such dosimeters were placed in a grid layout within the room, avoiding any obstructions and maintaining a 60 cm distance from surfaces. After a three-month exposure, chemical etching was performed (2.5 N NaOH at 60°C for 90 minutes), and track densities were analyzed using a spark counter. The CFD results showed a 13.5% relative deviation from passive monitoring and a 34.6% deviation from active monitoring, validating the CFD model's predictive capacity. While the study did not address the relationship between indoor environmental parameters and radon behavior, it remains among the earliest residential studies validating CFD for indoor radon dispersion.

In a more recent study, Adelikhah et al. (2023) explored indoor radon distribution in a naturally ventilated test room using CFD simulations and passive detectors. Solid-state nuclear track detectors (SSNTDs) such as Raduet and NRPB were used, with CR-39 detectors placed at heights of 0.2 m, 1.0 m (breathing zone), and 1.8 m. Detectors were located at least 20 cm from walls and were chemically etched (6.0 M NaOH at 90°C for 3 h) after 45 days of exposure. Track densities were analyzed using optical microscopy and image analysis software, with calibration conducted in radon chambers at the University of Pannonia, Hungary.

Active measurements were performed using AlphaGUARD PQ2000 PRO and RAD7 radon-thoron detectors. These instruments, operating on diffusion mode (60-minute cycles) and daily cycles respectively, also recorded temperature, humidity, and atmospheric pressure. Results revealed a negative correlation between radon levels and both humidity and ventilation rates. CFD simulations showed that increasing humidity from 30% to 50% resulted in a 5.8% increase in radon accumulation, suggesting humidity influences radon behavior, although this is likely affected by additional variables.

Akbari et al. (2013) investigated the effects of ventilation, temperature, and humidity on indoor radon using CFD simulations in ANSYS Fluent, alongside field measurements. Their case study featured an eight-room detached house in Stockholm equipped with a heat recovery ventilation. The CFD models was incorporated with air, moisture, and radon species with an air change rate of 0.25 ACH and radon levels around 600 Bq/m³ (originating from soil gas). They found that increasing humidity (30–70%) reduced radon due to moisture hindering diffusion. However, beyond 70%, denser air restricted radon movement, causing accumulation. Temperature variations between 15°C and 25°C had a minimal effect on radon levels, though a slight minimum was observed around 21°C, suggesting possible links to thermal comfort.

Rabi & Oufni (2017) also examined environmental influences on radon levels in a model house (100 m²) through numerical and experimental methods. Natural ventilation was provided via west- and east-facing windows. Their results showed a negative correlation between radon and humidity, and with temperature. Simulations considered temperatures from 15°C to 25°C and humidity levels from 30% to 80%. Findings revealed that increasing humidity reduced the diffusion coefficient, limiting radon transport and increasing concentration. Higher temperatures enhanced air dilution, reducing radon accumulation.

The reviewed literature demonstrates that radon concentration in indoor environments is influenced by multiple factors, including ventilation rates, humidity levels, temperature, building characteristics, and pressure differences. The interplay between humidity and radon accumulation remains an area requiring further exploration, particularly in Canadian residential settings in colder climates and closed room conditions. Future research should focus on refining CFD models with real-world measurement data to enhance the predictive accuracy of radon behavior under diverse environmental conditions.

Therefore, this study aims to investigate radon behavior in a Canadian residential indoor environment through both field measurements and numerical modeling by:

1. **Monitoring the indoor radon concentrations over a three-month winter period** using continuous radon detectors placed in a real residential setting, alongside with measurements of indoor temperature and humidity.

2. **Simulating the indoor radon dispersion** using Computational Fluid Dynamics (CFD) in ANSYS Fluent, incorporating measured environmental conditions such as temperature, relative humidity, and air change rates.
3. **Examining how varying thermal and ventilation conditions influence radon distribution** within the living space by analyzing simulation cases across different temperature and humidity scenarios.
4. **Validating simulation outcomes against measured data**, providing insights into the strengths and limitations of CFD modeling for indoor radon studies.

The methodology presented in Chapter 3 is designed to fulfill these objectives through a two-part approach: (1) a **field study** involving in-situ measurements in a detached home in Victoria, BC, and (2) a **numerical simulation study** that models radon behavior under varying environmental conditions.

Chapter 3 Methodology

This chapter details the materials and methods used in the study, including radon detectors, temperature, and humidity sensors, a case study house, and methods, including radon measurement, analytical analysis, and CFD simulation.

3.1 Case Study Overview

A single-family home, located in a suburban area of Victoria, BC, Canada, was selected due to its typical construction characteristics and age, representing many residential buildings in Canada. Built-in 1975 in compliance with the National Building Code of Canada, the house features a total floor area of approximately 250 m² in each of two stories, with construction details that include insulated drywall for walls, double-glazed windows, weatherproof exterior doors, and foundation in contact with the ground. These features contribute to the energy efficiency of the house, but they may also affect radon accumulation, especially during the heating season when ventilation rates are reduced.

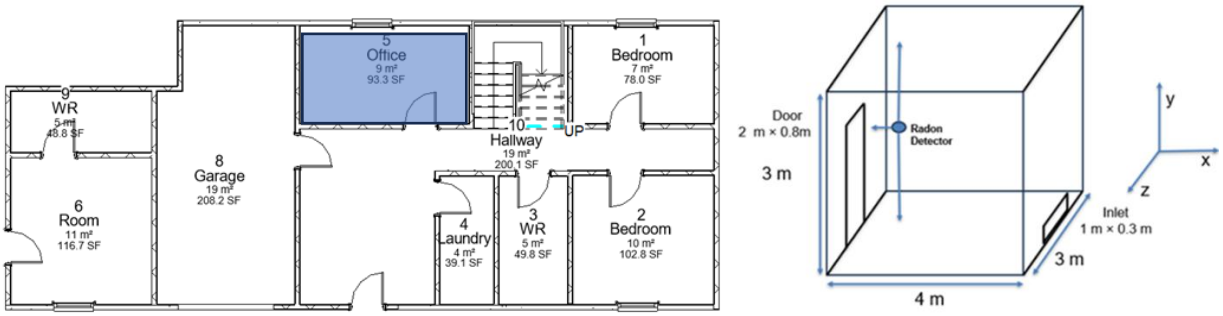

Figure 1: Floor Plan and Room Geometry for Radon Dispersion Analysis

This study focuses on one of the most frequently occupied rooms in the house, measuring 4.00 × 3.00 × 3.00 meters. This room was chosen based on the homeowner's request, as it is the most utilized space, making it an ideal setting to monitor radon exposure under typical living conditions. Additionally, the room is located on the lower level of the building, with its floor in direct contact with the soil, The room lacks mechanical ventilation, relying solely on natural air ventilation for

airflow, and baseboard heating for temperature controls which makes it particularly suitable for studying radon behavior in a confined indoor environment. The choice of this room is crucial for understanding how radon concentrations vary in commonly used indoor spaces, allowing the research to generate practical insights into radon mitigation strategies applicable to Canadian residential buildings.

3.2 Radon Measurement Procedure

To capture accurate radon concentration levels, a systematic radon measurement study was established over six-week period during the heating season, from November to December. This timeframe was selected because radon levels tend to be higher during colder months when windows and doors remain closed, leading to reduced natural ventilation.

3.2.1 Detector Placement and Monitoring

A continuous radon detector EcoQube manufactured by EcoSense, employing pulsed chamber technology to provide high sensitivity and real-time measurement capabilities was used for the radon testing. The detectors were on a raised table near to the entrance to the room , specifically at 1 meter from the wall, 1 meter from the ground, and 1 meter from the ceiling, ensuring the radon detector were positioned within the breathing zone. There was only one radon detector placed in the room, this is because the EcoQube detector features a measurement range of 0.2 to 99.9 pCi/L (7 to 3,700 Bq/m³) and utilizes patented radon detection technology with industry-leading sensitivity of 30 counts per hour per pCi/L. It provides the first reading within 10 minutes, with highly reliable results available within 60 minutes. The detector continuously measures radon concentration in the room, recording data every 10 minutes and providing hourly and daily averages, making it an exceptionally practical tool for indoor radon testing.

This sensor placement ensured an accurate representation of the radon concentrations that occupants would typically be exposed to by positioning the detector within the breathing zone and minimizing the potential influences from localized air circulation patterns, nearby objects, and occupant activities. In addition to the radon concentration detector, a temperature and humidity sensor was installed near the radon monitor in the room to measure indoor environmental

conditions. Figure 1 shows the location of the radon detector and the temperature and humidity sensor in the room, and Figure 2 shows the radon detector used in the room for radon testing.

3.2.2 Data Collection and Analysis

Radon concentrations were recorded every 10 minutes, with data reported as 60-minute moving averages to smooth out short-term fluctuations and capture long-term trends. This high-resolution monitoring approach enabled the identification of peak radon levels, diurnal variations, and responses to changes in temperature, humidity, or ventilation. Outdoor weather data, including temperature, humidity, and wind speed, were collected from a nearby weather station to provide context on how external conditions might affect indoor radon levels.

The collected data were then subjected to continuous statistical analysis, allowing for the identification of patterns, trends, and correlations between indoor radon concentrations and environmental factors. This analysis formed the foundation for calibrating the CFD model, ensuring that simulation results closely matched real-world observations.

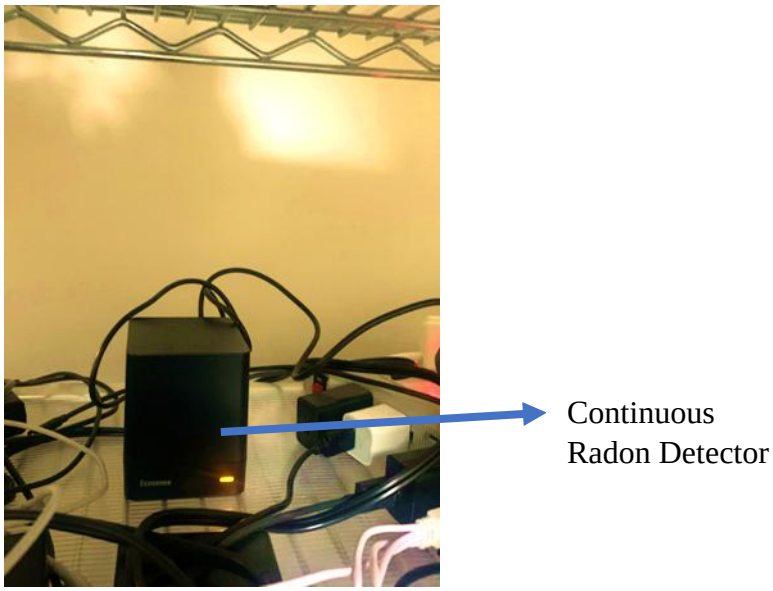

Figure 2: Placement of Eco-Cube Continuous Radon Detector in the Test Room

The study employed an analytical approach to calculate indoor radon concentrations based on fundamental factors, including the radon exhalation rate, decay rate, ventilation rate, room volume, and surface area. This approach facilitated the validation of measurement data and helped identify potential discrepancies which will be discussed in the next chapter.

3.3 CFD Analysis

This section presents the computational fluid dynamics (CFD) analysis conducted to investigate the flow field, radon dispersion, and the impact of environmental factors such as temperature, humidity, and ventilation rates on indoor air quality within the simulated domain.

3.3.1 Geometry and Domain Configuration

The CFD simulations were conducted using ANSYS Fluent to replicate the selected room's geometry, capturing realistic indoor conditions. The computational domain was modeled as a rectangular prism with dimensions reflecting the test room (4 m × 3 m × 3 m). Additional features, such as a human model and furniture, were incorporated to simulate typical occupancy and investigate radon exposure at different breathing heights. The inlet A has a measurement of 1m x 0.7 m and outlet B was considered the gap between the floor and the door.

The floor was modeled with light concrete, while the walls used dense concrete, representing materials commonly found in residential construction. These properties, such as density, thermal conductivity, and permeability, were carefully selected based on literature values to accurately simulate radon diffusion and interaction within the room.

Table 1 summarizes the properties of all materials used in this study, including air, water vapor, radon, light concrete, and dense concrete. These properties were carefully chosen based on literature values and adjusted to match real-world conditions as closely as possible, ensuring that the simulation results were both accurate and reliable.

The ceiling was defined as an adiabatic boundary, meaning it was assumed to have no heat transfer. This simplification helped reduce computational complexity in the thermal analysis. The basic concept of this project is to consider the floor as the radon source, while the air entering through

the inlet, carrying specific temperature and humidity conditions, facilitates radon dispersion within the room. After allowing the radon to disperse under these conditions, readings were taken for analysis

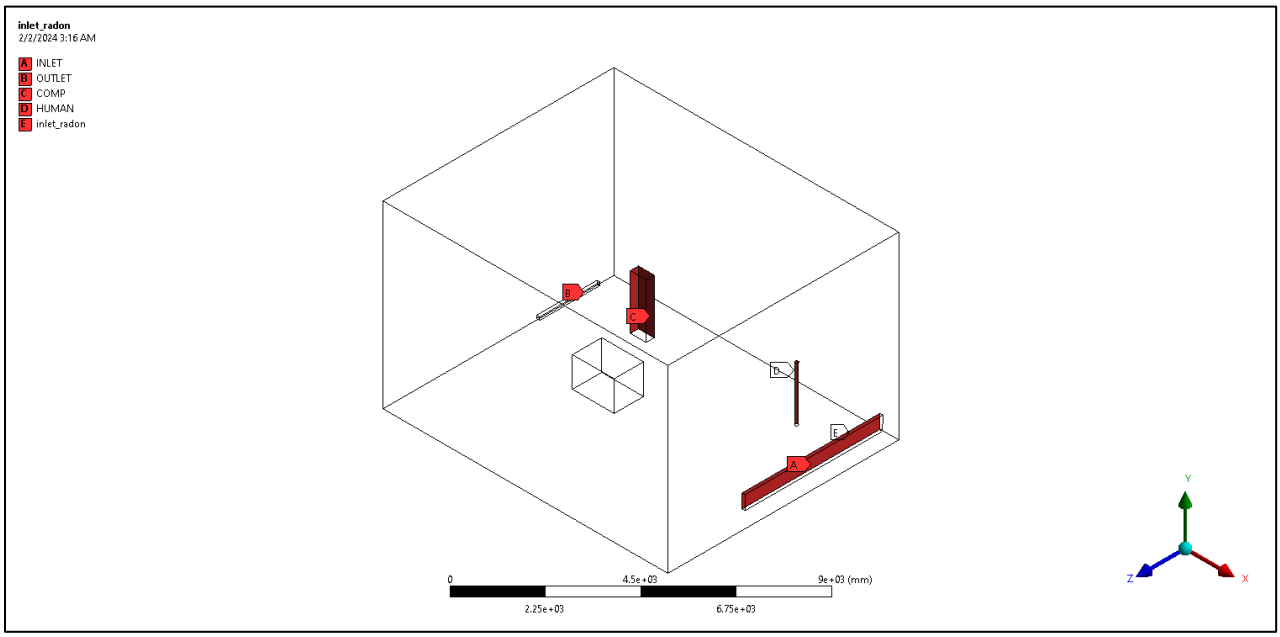

Figure 3: 3D Room Geometry Developed in ANSYS Fluent R2

Table 1: Properties of the materials used in the simulation

Property	**Air**	**Water Vapor**	**Radon**	**Light Concrete**	**Dense Concrete**
Density (kg/m³)	1.225	0.5542	9.73	1200	2100
Specific Heat Cp (J/kg K)	1006.43	2014	96.35	1000	840
Thermal Conductivity K (W/m K)	0.0242	0.026	0.0036	0.4	1.4
Viscosity (kg/ms)	1.7894×10^{-5}	1.34×10^{-5}	1.8×10^{-5}	-	-

Molar Weight **MW (kg/k mol)**	28.966	18.0153	222	-	-

3.3.2 Meshing Strategy and Grid Independence Test

An effective meshing strategy is crucial for ensuring the accuracy and efficiency of CFD simulations. The study employed a hybrid meshing approach with 1529023 elements, combining structured and unstructured mesh elements:

- **Structured Mesh:** Applied to the main room geometry, providing uniform cell distribution and numerical stability.
- **Unstructured Mesh:** Used around complex features such as the human model, table, and ventilation openings, allowing better adaptation to irregular geometries.

A grid independence test was performed to ensure that further mesh refinement did not significantly alter the simulation results, confirming that the chosen mesh resolution was sufficient for capturing essential details of radon transport and distribution. Three different mesh resolutions were tested to analyze radon transport and distribution without incurring excessive computational costs: a) the Coarse Mesh, consisting of approximately 50,000 elements; b) the Medium Mesh, with 150,000 elements; and c) the Fine Mesh, comprising 300,000 elements. Simulations were performed under identical boundary conditions, including radon exhalation rate, ventilation rate, temperature, and humidity. Radon concentrations were recorded at key locations including the inlet area, breathing zone and outlet. The difference in radon concentration between the Medium and Fine meshes was less than 2%, demonstrating that further refinement did not significantly alter the results. The computational time for the medium mesh was approximately 40% shorter than that of the Fine mesh. Based on the findings, the Medium Mesh (~150,000 elements) was selected for subsequent simulations. A combination of medium and fine meshes was utilized to create the overall meshing strategy as it provided a good balance between accuracy and computational cost, ensuring reliable results while optimizing resource usage.

Table 2: Grid Independent Test Result

Mesh Resolution	Element Size (m)	Location 1 (Bq/m³)	Location 2 (Bq/m³)	Location 3 (Bq/m³)	Relative Error (%)
Coarse Mesh	0.5	22.5	18.0	15.5	-
Medium Mesh	0.25	22.1	17.8	15.3	2.0
Fine Mesh	0.1	22.0	17.7	15.2	0.5

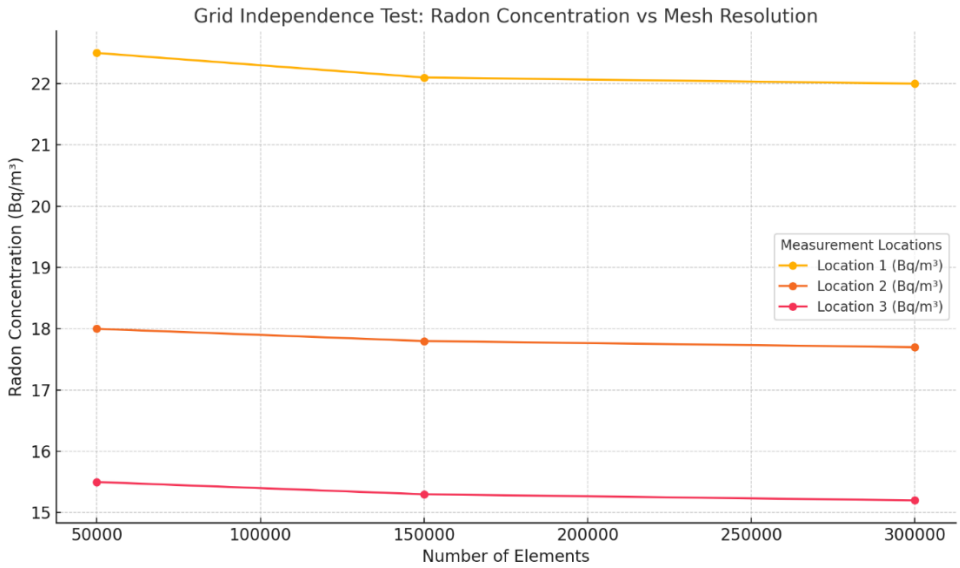

Figure 4: Grid Independence test with radon concentration and mesh resolution

3.3.3 Assumptions

The air change rate (ACH) in the simulated building was set at 0.5 ACH, reflecting the absence of mechanical ventilation in the case study house. This value was chosen based on findings from previous studies that examined similar residential buildings under comparable conditions. The chosen ventilation rate directly influenced the radon dispersion and indoor air quality analysis. By simulating airflow at 0.5 ACH, the study provides a realistic representation of the building's actual ventilation performance and its impact on radon transport.

3.3.4 Boundary Conditions

Accurate boundary conditions are essential for replicating real-world scenarios. The study established the following conditions:

- **Inlet Boundary:** Air entered the room at a specified ventilation rate of 0.5 ACH^{-1}, with the inlet velocity calculated based on the room's volume and ventilation area. The inlet velocity corresponding to the ventilation rate and the ventilation area was calculated from Eq. (3.1).

$$v = \frac{ACH \times Vroom}{Avent} \qquad eq\ 3.1$$

  The air change rate was set at 0.5 ACH^{-1}, reflecting typical residential ventilation standards. The occupied air volume in the test room was considered as the room volume (Vroom), which was 36 m^3, corresponding to the room dimensions of 4 meters in length, 3 meters in width, and 3 meters in height. The ventilation area (A_{vent}) in the closed room condition was the opening in the wall, measuring 0.3 m^2. The inlet velocity required to achieve this air change rate in the room is approximately 0.01667 m/s,

- **Outlet Boundary:** An outflow boundary condition allows air and radon to exit the room, facilitating a continuous flow that resembles typical ventilation.
- **Wall and Floor Conditions:** No-slip conditions were applied to the walls, floor, and ceiling, ensuring that air velocity at these surfaces was zero. The radon exhalation rate was set to match the measured values, ensuring an accurate representation of radon entry from the floor.

3.3.5 Turbulence Modeling and Solver Settings

The k-ω Shear Stress Transport (SST) turbulence model was selected due to its ability to handle complex flow phenomena and predict turbulent behavior near walls. This model is well-suited for indoor air quality studies, as it accurately captures the impact of airflow on radon dispersion.

The energy model was activated to simulate thermal effects within the room, allowing the study to analyze how temperature gradients influenced radon behavior. ANSYS Fluent's finite volume solver was used to discretize and solve the governing equations iteratively, ensuring a high degree of accuracy in the simulation results.

3.4 Calibration and Validation of CFD Model

The CFD model was calibrated using the real-world radon measurements taken from the case study house. Calibration involved adjusting parameters such as the radon exhalation rate, diffusion coefficient to ensure that the simulation results closely matched observed data. This calibration process was critical for enhancing the model's predictive capabilities, ensuring that it accurately represented the dynamics of radon transport in the indoor environment.

Chapter 4 Results and Observations

This chapter presents the results obtained from the study, including measurement data, analytical results, and numerical simulation results of the indoor radon concentration in the test room.

4.1 Radon Measurement

Radon concentration measurements were carried out in the selected room over six weeks, during the heating season (November to December). A continuous radon monitor, along with temperature and humidity sensors, was used to collect data, ensuring an accurate representation of radon behavior under real-world conditions. During this period, the indoor environment was maintained with closed windows and doors, simulating a worst-case scenario where radon could accumulate without interference from external air exchange. This controlled setting allowed for a clearer assessment of how environmental factors such as temperature and relative humidity influence radon levels.

4.2 Radon Measurement Results

Radon concentration, temperature, and relative humidity were monitored hourly over a six-week period from November 8 to December 20, 2023. The average radon concentration recorded was 16.8 Bq/m³, which is well below Health Canada's recommended threshold of 200 Bq/m³. During the same period, the average indoor temperature was 20.3°C, and the average relative humidity was 40.5%. Figure (5a) represents the hourly time series data for temperature and humidity throughout the monitoring period, and Figure (5b) presents the hourly time series data for temperature and radon throughout the monitoring period. The x-axis displays the date and time, while the y-axis represents temperature (orange) and the right y-axis shows relative humidity (yellow). In Figure 5b, the y-axis represents the radon concentration (green), and the right y-axis shows temperature (orange).

Temperature remained relatively stable, generally fluctuating between 18°C and 22°C, indicating a well-regulated indoor environment due to active space heating during the colder season. In

contrast, humidity showed greater variability, ranging from approximately 35% to 51%, with a noticeable drop in early November before stabilizing mid-month.

Radon concentrations exhibited more significant fluctuations compared to temperature and humidity. Notable spikes were observed in early December, with the maximum recorded value reaching 83 Bq/m³, while the lowest hourly values were around 7 Bq/m³. These fluctuations are likely influenced by dynamic environmental and ventilation factors, including variations in air leakage, pressure differentials, and occupant behavior. Although a direct statistical correlation between radon and environmental variables was not computed, the data suggests that radon peaks may align with periods of lower humidity, possibly due to increased soil gas infiltration or changes in radon diffusion properties under drier conditions.

While temperature remained relatively constant, radon concentrations showed a more dynamic pattern, due to the influence of air movement driven by the stack effect.

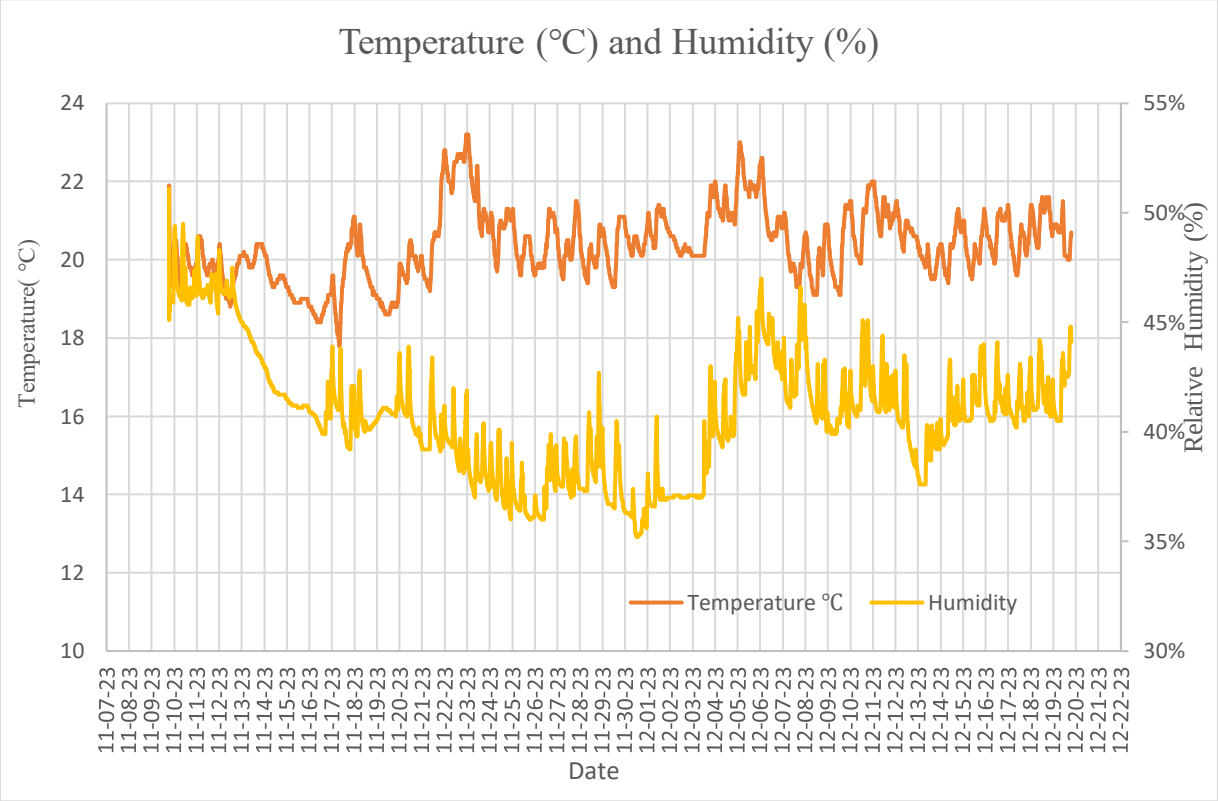

(a)

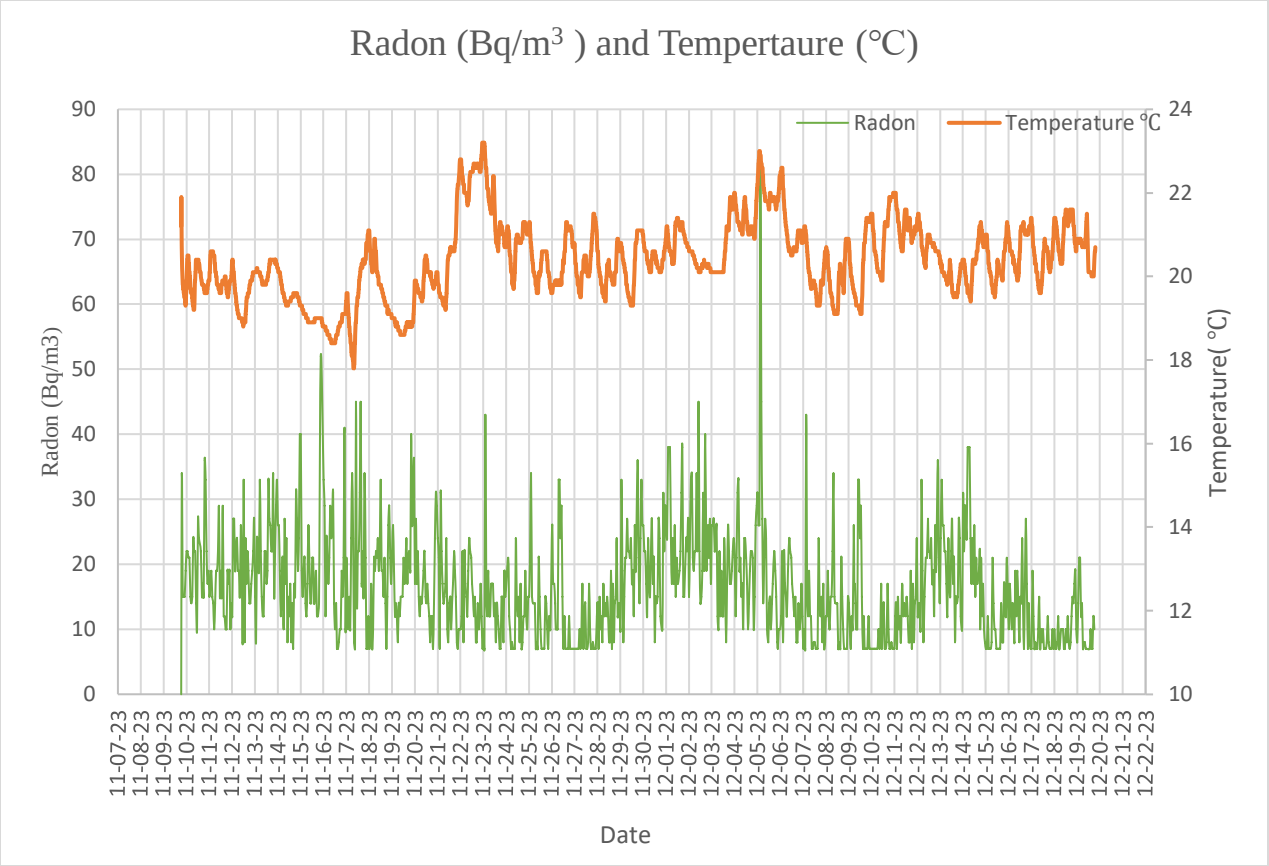

(b)

Figure 5: (a) Hourly measurement of temperature (°C) and Humidity (%) recorded during the test period; and (b) Hourly measurement of radon (Bq/m³) and temperature (°C) recorded during the test period

4.3. Radon Concentration Calculation

The radon exhalation rate was determined using the measured data, and the following analytical equation was employed to calculate indoor radon concentration. For the input parameters, the radon concentration C is calculated using *eq 4.1(Adelikhah et al., 2023; Akbari et al., 2013)*

$$C = \frac{Ei \,.\, Ai}{(\lambda o + \lambda v) \,.\, Vroom} \qquad eq\ 4.1$$

In this formula, **C** represents the radon concentration (Bq/m³), Ei is the radon exhalation rate (Bq/m²·h), **A** is the exhalation area (m²), $\boldsymbol{\lambda_o}$ is the radon decay constant (s^{-1}), $\boldsymbol{\lambda_v}$ is the ventilation rate in (s^{-1}), and $\mathbf{V_{room}}$ is the room volume (m³).

From the experimental analysis, the radon concentration **C** is 16.80 Bq/m³, the room of volume ($\mathbf{V_{room}}$) is 36 m³, and radon decay constant ($\boldsymbol{\lambda_o}$) of $2.11\times10^{-6}s^{-1}$.

The ventilation rate (λ_v),

$$\lambda_v = \frac{ACH}{3600} \qquad \textit{eq 4.2}$$

The ventilation rate was 1.39×10^{-4} (corresponding to an ACH of 0.5 ACH^{-1}), and the radon exhalation rate (Ei) was found approximately 0.007 Bq/m²·s, or 25.2 Bq/m²·h. The rate of radon is used as an input parameter in the CFD code, a rate at which radon is generated from the floor

4.4 Numerical Simulation Results

The numerical simulation, conducted using ANSYS Fluent, aimed to replicate real-world indoor conditions and analyze the impact of temperature, humidity, and ventilation on radon concentration. Since environmental factors significantly influence indoor radon levels, it is essential to examine the combined effects of temperature, humidity, and ventilation. Computational Fluid Dynamics (CFD) provides a robust method to visualize and evaluate how these parameters interact and affect radon distribution in indoor environments.

To investigate these interactions, nine simulation cases were selected based on observed environmental conditions. Temperatures of 18°C, 21°C, and 24°C were chosen to represent the lowest, median, and highest recorded values, respectively. Likewise, relative humidity levels of 20%, 40%, and 60% were selected to reflect the lowest, median, and highest observed humidity levels. All simulations were conducted at a constant air change rate of 0.5 ACH.

Radon concentrations were analyzed at two different heights: at the floor level and at 2 meters, representing the typical human breathing zone. These simulations provided valuable insights into radon dispersion patterns under varying environmental conditions. Table 4 summarizes the input

parameters used in the simulations, including variations in temperature (T), relative humidity (RH), and air change rate (ACH). Each case is labeled from N1 to N9, corresponding to a specific combination of environmental factors. These cases are discussed individually in the following sections, along with the corresponding radon concentration plots.

Table 3: Case number and parameters

Case no	Parameter Change
N1	T=18℃, RH=20%, ACH=0.5^{-1}
N2	T=21℃, RH=20%, ACH=0.5^{-1}
N3	T=24℃, RH=20%, ACH=0.5^{-1}
N4	T=18℃, RH=40%, ACH=0.5^{-1}
N5	T=21℃, RH= 40%, ACH=0.5^{-1}
N6	T=24℃, RH= 40%, ACH=0.5^{-1}
N7	T=18℃, RH= 60%, ACH=0.5^{-1}
N8	T=21℃, RH= 60%, ACH=0.5^{-1}
N9	T=24℃, RH= 60%, ACH=0.5^{-1}

4.4.1 Case N1, Low Temperature (18°C) and Low Humidity (20%) Condition.

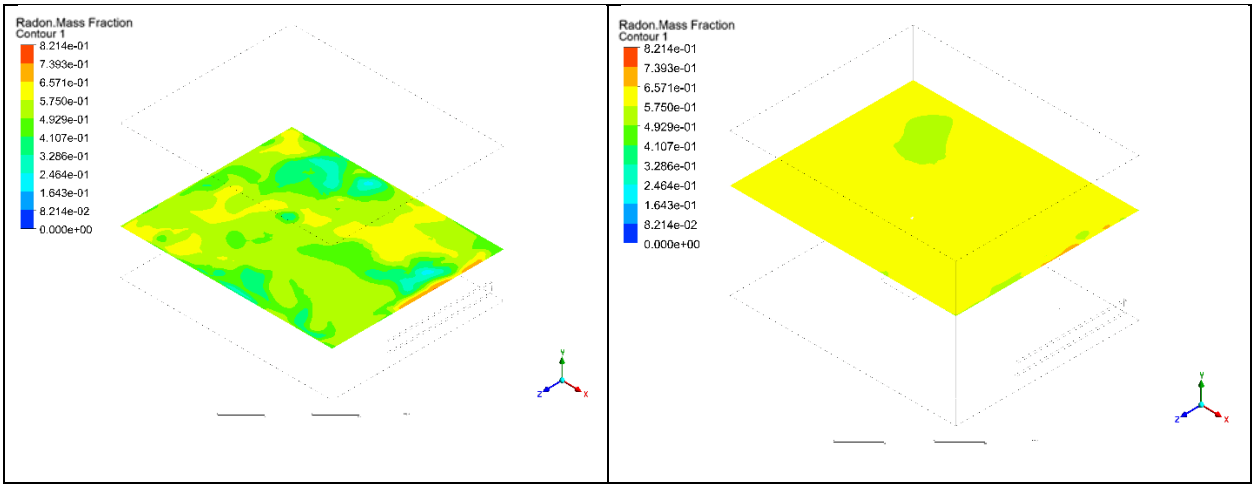

Figure 6: Radon Concentration Distribution at 60 Seconds: Case N1 at T= 18℃, RH=20%, ACH=0.5^{-1} (Lower breathing zone (left) and Upper breathing zone (right)

The simulation results for the case condition of 18℃ and 20% RH showed that radon concentrations were higher near the floor, as expected due to the higher radon density. However, more radon levels were also observed near the ceiling, indicating that air circulation, driven by stack effect was strong enough to transport radon upwards. This upward movement suggests that under low temperature and low humidity conditions, radon tends to disperse more uniformly throughout the room, with significant presence in the breathing zone.

4.4.2 Case N2, Moderate temperature (21°C) and low humidity (20%) Condition.

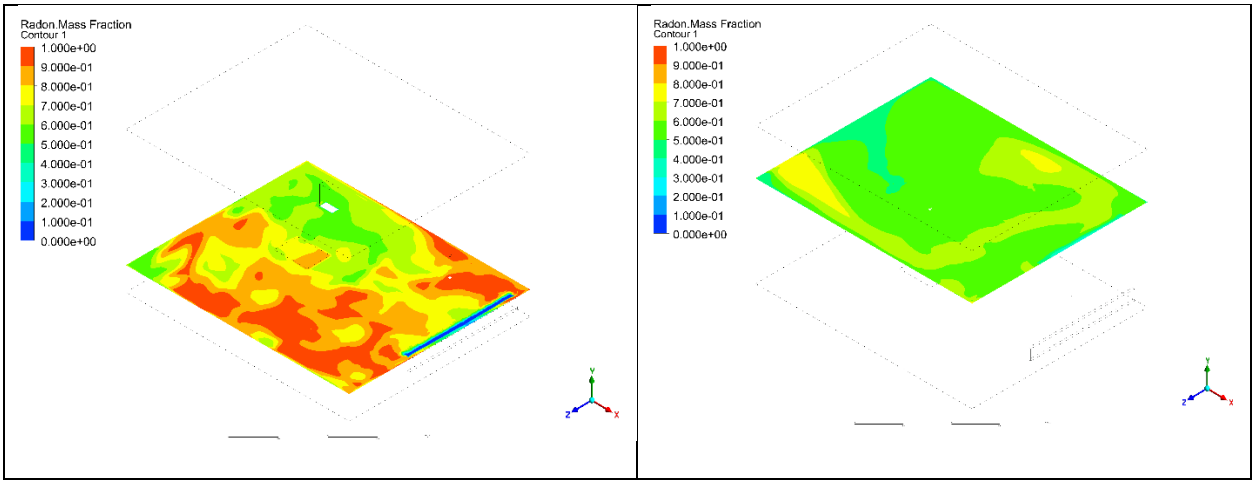

Figure 7: Radon Concentration Distribution at 60 Seconds: Case N2 at T= 21℃, RH=20%, ACH=0.5^{-1} (Lower breathing zone (left) and Upper breathing zone (right)

At a moderate indoor temperature of 21°C with low relative humidity (20%), radon diffusion into the indoor environment slightly increases compared to the lower temperature condition (Case N1). Diffusion is the process by which particles move from areas of high concentration to low concentration. In this case, the moderate temperature in the control volume promoted radon from the floor, contributing to higher concentrations within the space.

The elevated radon levels are noticeable in areas farther from the outlet, where air circulation is weaker. Additionally, the low humidity condition continues to favor radon mobility, as dry air presents fewer barriers to diffusion. As a result, radon concentrations under these conditions are higher compared to scenarios with greater humidity.

4.4.3 Case N3, Elevated temperature (24°C) and low humidity (20%) condition

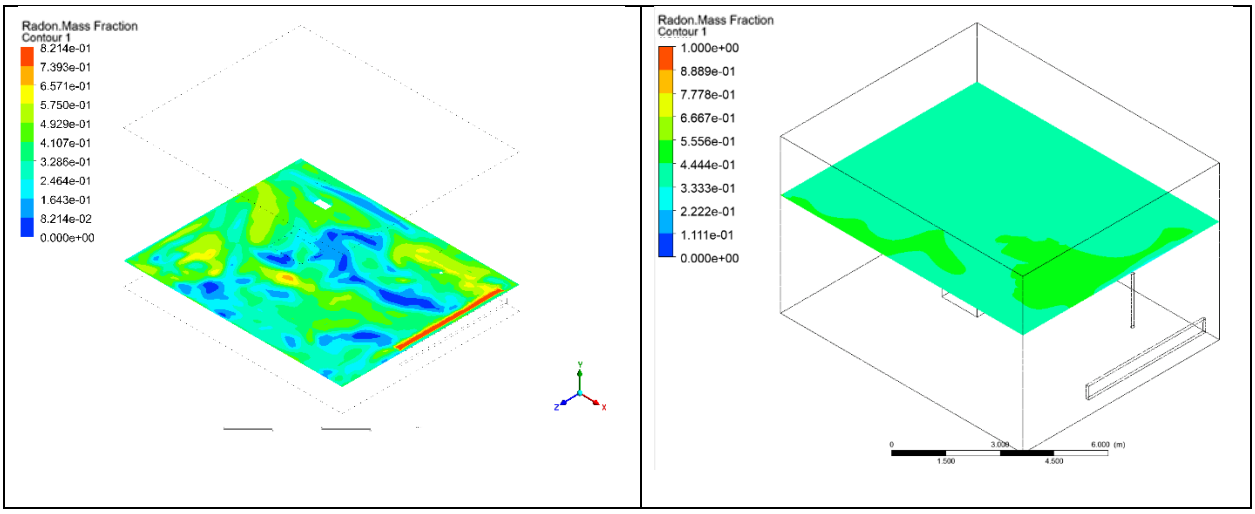

Figure 8: Radon Concentration Distribution at 60 Seconds: Case N3 at T= 24℃, RH=20%, ACH=0.5^{-1}

At a higher indoor temperature of 24°C, the radon from the ground is expected to increase due to advection from the ground. Additionally, the low relative humidity (20%) favors radon diffusion, as dry air allows radon to move more freely compared to humid conditions.

However, the simulation results revealed an unexpected outcome as the overall radon concentration was significantly reduced at the floor and ceiling level compared to the previous temperature condition at 21°C (Case N2). The contour plot shows that in certain regions of the

room, radon levels were observed to be near zero. This outcome suggests that the combined effect of elevated temperature, low humidity, and a ventilation rate of 0.5 ACH^{-1} (air changes per hour) enhanced the air movement and dilution of radon and prevented radon from building up within the space.

4.4.4 Case N4, Low Temperature (18°C) and Moderate Humidity Levels (40%)

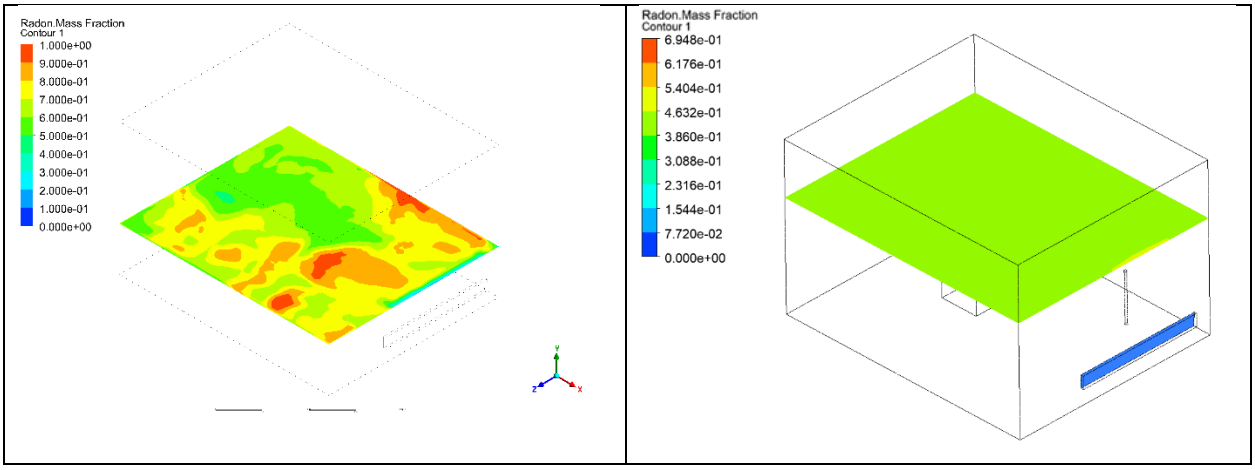

Figure 9: Radon Concentration Distribution at 60 Seconds: Case N4 at T= 18℃, RH=40%, ACH=0.5^{-1} (Lower breathing zone (left) and Upper breathing zone (right)

At a relatively low indoor temperature of 18°C, radon gas, being denser than air, tends to accumulate closer to the floor. In this scenario, the balance between low temperature and moderate humidity creates conditions that favor radon accumulation near the to the floor level of the room, compared to the ceiling level.

4.4.5 Case N5, Moderate Temperature (21°C) and Moderate Humidity (40%) condition.

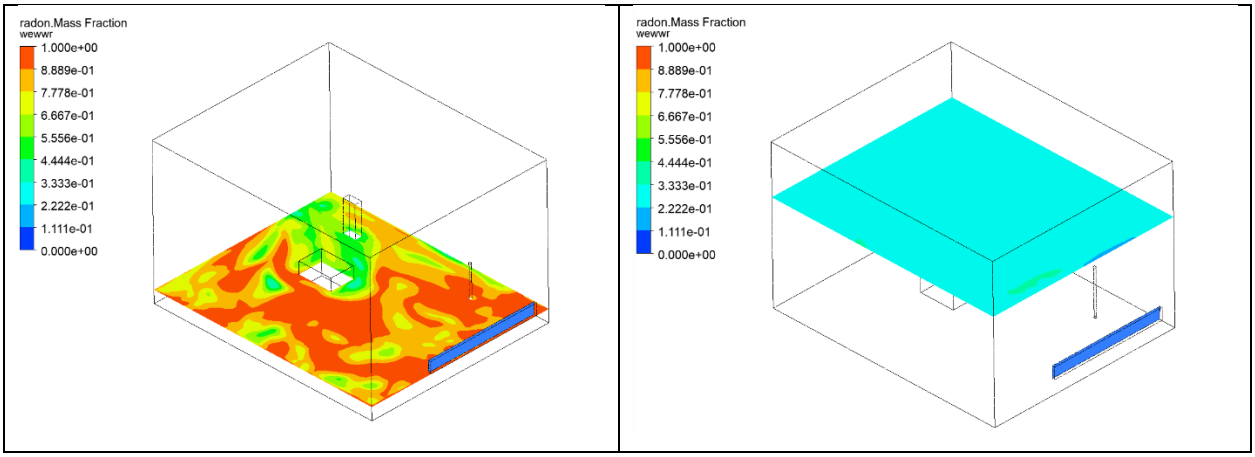

Figure 10: Radon Concentration Distribution at 60 Seconds: Case N5 at T= 21℃, RH=40%, ACH=0.5^{-1} (Lower breathing zone (left) and Upper breathing zone (right)

This case is particularly important in the study, as the temperature and humidity conditions (21°C and 40% RH) closely match the average measurement in the case study house. The simulation contours showed that increased radon concentration was present throughout most of the room, with the exception of areas near the outlet, suggesting that a temperature-driven airflow pattern was established within the space. This pattern suggests the development of a temperature-driven airflow that facilitated the movement of warmer indoor air and radon toward the outlet.

Radon concentration near the floor was consistently higher than at the ceiling, which aligns with the natural behavior of radon as a heavy gas. This case also recorded the highest radon concentration at floor level among the simulations conducted at 40% relative humidity. In contrast, the radon concentration near the ceiling was significantly lower, indicating more effective air exchange between the indoor and outdoor environments in the room, which helped to reduce radon from the zone.

4.4.6 Case N6, Elevated temperature (24°C) and moderate humidity (40%)

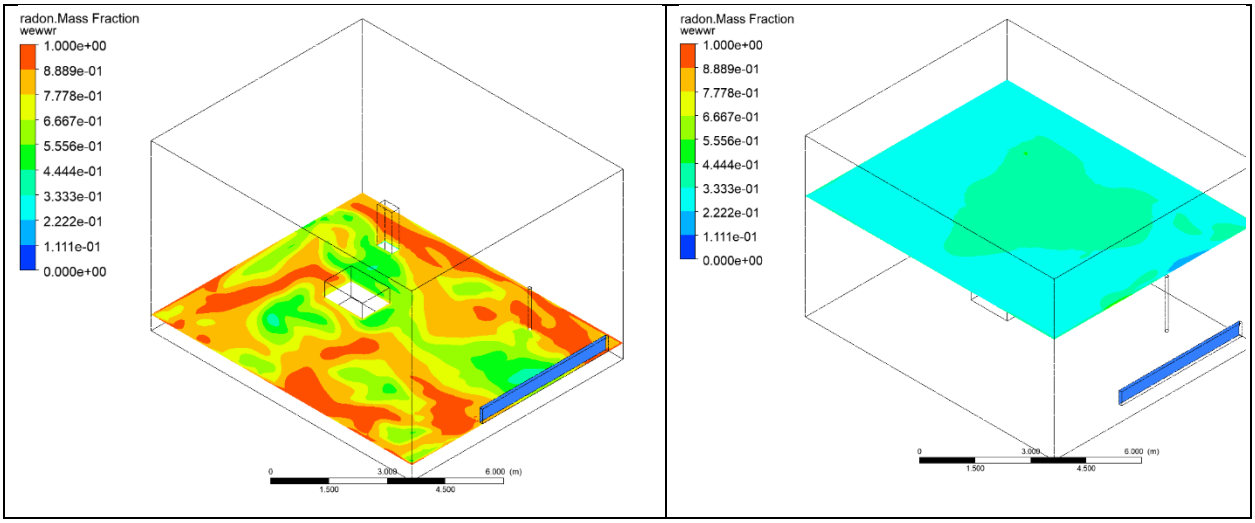

Figure 11: Radon Concentration Distribution at 60 Seconds: Case N6 at T= 24°C, RH=40%, ACH=0.5^{-1} (Lower breathing zone (left) and Upper breathing zone (right))

At 24°C, a relatively warm indoor temperature, radon gas becomes more mobile and diffusive due to increased thermal energy. This heightened molecular activity enhances radon exhalation from the floor, resulting in greater radon release into the indoor environment compared to cooler conditions. Additionally, the warmer temperature promotes buoyancy-driven airflow, leading to stronger air circulation throughout the space. As a result, radon concentrations tend to be higher near the ceiling area at 24°C (N6) compared to the 21°C (N5) case.

4.4.7 Case N7, Low Temperature (18°C) and High Humidity (60%) condition.

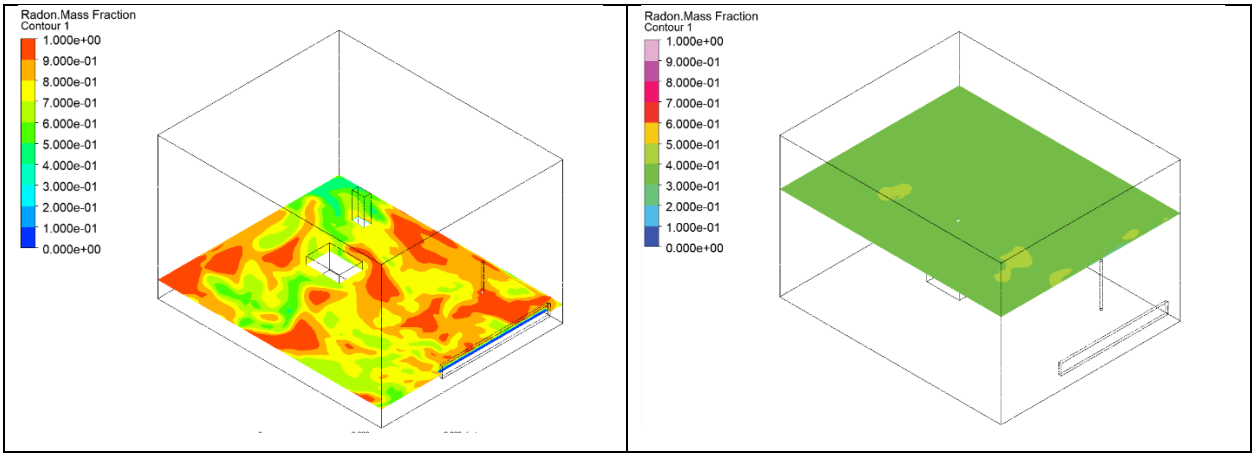

Figure 12: Radon Concentration Distribution at 60 Seconds: Case N7 at T= 18°C, RH=60%, ACH=0.5^{-1} (Lower breathing zone (left) and Upper breathing zone (right)

Under conditions of low temperature (18°C) and high relative humidity (60%), the results indicated a notable accumulation of radon, particularly near the floor where it is initially released. The simulation revealed that this scenario recorded the highest radon concentration across all floor-level cases. This can be explained by the elevated humidity levels in the room, which contribute to increased radon emanation, causing radon to concentrate closer to the ground. Although some radon disperses to higher elevations within the room, the dominant accumulation remains near the floor.

4.4.8 Case N8, Moderate temperature (21°C) and high humidity (60%) condition

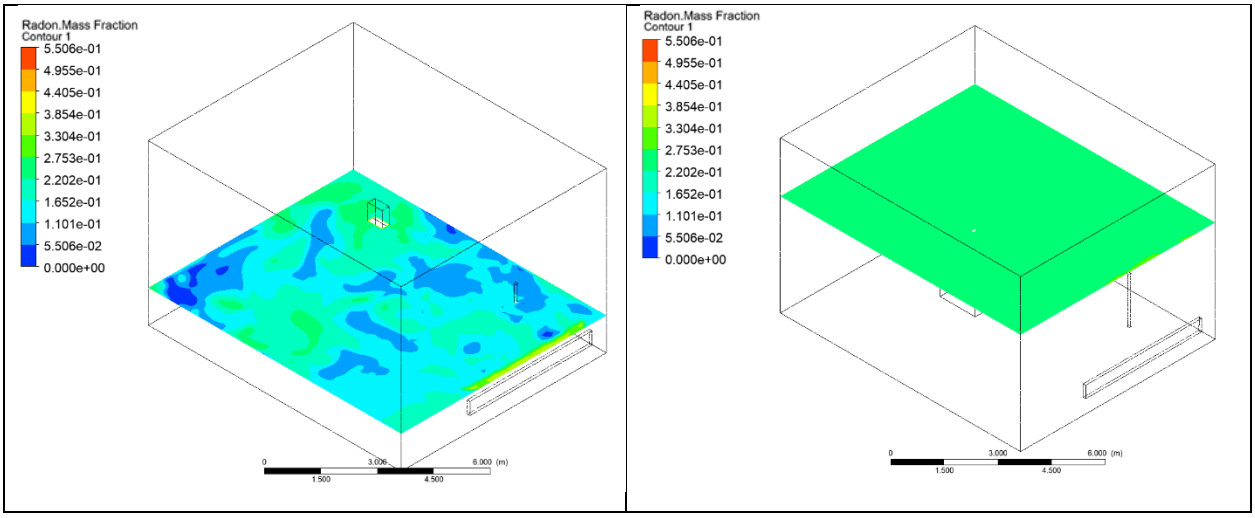

Figure 13: Radon Concentration Distribution at 60 Seconds: Case N8 at T= 21℃, RH=60%, ACH=0.5^{-1} (Lower breathing zone (left) and Upper breathing zone (right)

In this scenario, the indoor temperature is maintained at a moderate 21°C, while the relative humidity is elevated to 60%. The simulation results indicate that radon concentration at the floor level is lower compared to the concentration near the ceiling. This pattern is attributed to the high moisture content in the air; water molecules effectively act as a barrier, reducing the diffusion and upward movement of radon from the source at the floor level. Additionally, the moderate temperature contributes to promoting natural airflow and enhancing the exchange between indoor and outdoor air.

4.4.8 Case N9, Moderate temperature (24°C) and high humidity (60%) condition

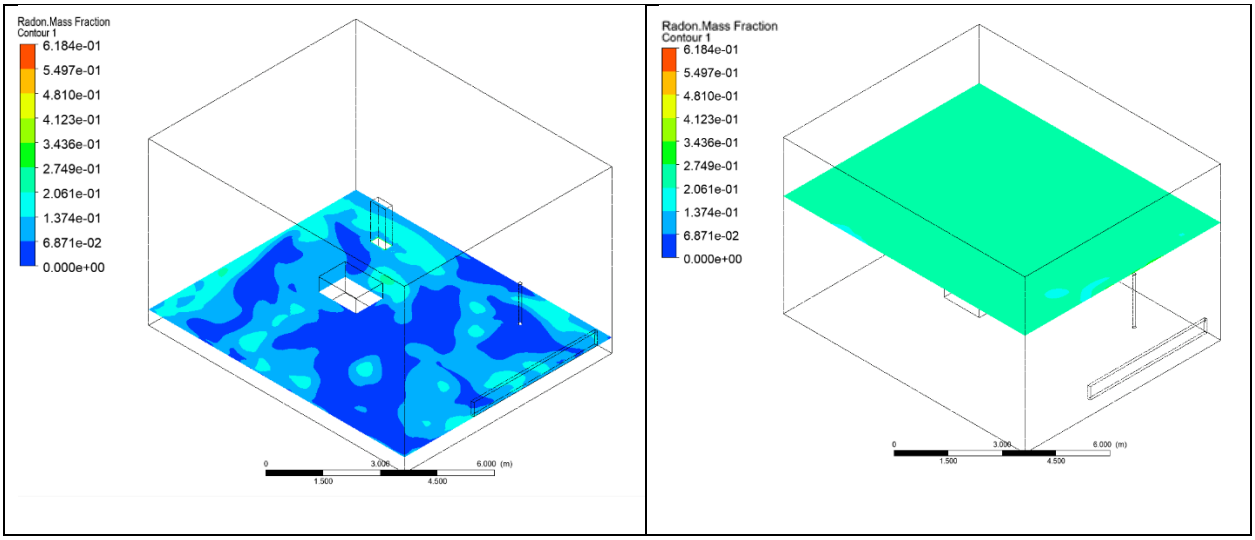

Figure 14: Radon Concentration Distribution at 60 Seconds: Case N1 at T= 24℃, RH=60%, ACH=0.5^{-1} (Lower breathing zone (left) and Upper breathing zone (right)

In this case, the presence of high relative humidity (60%) played a significant role in reducing radon concentrations. Despite the favorable temperature for radon release, the high moisture content in the air likely acted as a barrier, limiting the emission and mobility of radon from the floor and reducing its overall presence in the room.

As a result, radon concentrations were significantly lower than expected, with this case recording the lowest radon levels across all simulations. The concentration near the floor was particularly low, with even lower levels observed at the ceiling, further indicating effective suppression of radon transport under these conditions. This outcome highlights the complex interaction between temperature, humidity, and air movement, demonstrating that while warm temperatures can promote radon release, high humidity can substantially counteract this effect, reducing overall indoor radon levels.

Table 4: Average Radon Mass Fraction from the case study

Parameters	**Radon mass fraction in Lower breathing zone (%)**	**Radon mass fraction in Upper breathing zone (%)**
T=18°C, RH=30%, ACH=0.5 ACH^{-1}	0.54	0.61

T=21°C, RH=30%, ACH=0.5 ACH^{-1}	0.81	0.70
T=24°C, RH=30%, ACH=0.5 ACH^{-1}	0.41	0.44
T=18°C, RH=40%, ACH=0.5 ACH^{-1}	0.78	0.38
T=21°C, RH=40%, ACH=0.5 ACH^{-1}	0.88	0.22
T=24°C, RH=40%, ACH=0.5 ACH^{-1}	0.77	0.34
T=18°C, RH=50%, ACH=0.5 ACH^{-1}	0.91	0.31
T=21°C, RH=50%, ACH=0.5 ACH^{-1}	0.16	0.27
T=24°C, RH=50%, ACH=0.5 ACH^{-1}	0.06	0.20

The table provides data on radon concentrations at both the lower breathing zone and upper breathing zone under varying temperature (T), relative humidity (RH), and air change rate (ACH) conditions. As the temperature increased from 18°C to 24°C, radon levels generally decreased at both the floor and ceiling. The effect of humidity is more pronounced: at low humidity (20%), radon concentrations were higher, particularly at 21°C, but significantly decreased as humidity increased to 60%.

Table 5: Average Radon Bq/m3 from the case studies

Parameters	**Radon concentration in lower breathing zone (Bq/m^3)**	**Radon Concentration in Upper breathing zone (Bq/m^3)**
T=18°C, RH=20%, ACH=0.5 ACH^{-1}	11.03	12.45
T=21°C, RH=20%, ACH=0.5 ACH^{-1}	16.54	14.29
T=24°C, RH=20%, ACH=0.5 ACH^{-1}	8.37	8.98
T=18°C, RH=40%, ACH=0.5 ACH^{-1}	15.93	7.76
T=21°C, RH=40%, ACH=0.5 ACH^{-1}	17.97	4.49

T=24°C, RH=40%, ACH=0.5 ACH^{-1}	15.72	6.94
T=18°C, RH=60%, ACH=0.5 ACH^{-1}	18.58	6.33
T=21°C, RH=60%, ACH=0.5 ACH^{-1}	3.27	5.51
T=24°C, RH=60%, ACH=0.5 ACH^{-1}	1.23	4.08

The highest radon levels were observed at 18°C with 60% humidity, while the lowest radon concentrations occurred at 24°C with 60% humidity, indicating that both higher temperatures and humidity levels are effective in reducing radon presence, with more uniform radon distribution and less accumulation at higher levels of these variables. This trend emphasizes the importance of maintaining adequate indoor temperature and humidity for radon mitigation.

Based on the data, the optimal indoor temperature for residents, considering radon concentration management, appears to be **21°C- 24°C**. At this temperature, combined with a relative humidity of **40-60%**, the radon concentration was significantly lower at both the floor and ceiling levels compared to other temperature and humidity combinations. This suggests that maintaining an indoor environment around **21°C- 24°C** with high humidity **40-60%** creates conditions that effectively reduce radon levels, ensuring safer indoor air quality. Additionally, this temperature is comfortable for most residents, making it ideal for maintaining both health and comfort within the living space.

4.5 Model Validation

To validate the numerical simulation results, a comparison was made between measured radon concentrations, analytical calculations, and CFD simulation outcomes

Table 6: Model validation using analytical calculation and numerical simulation.

ACH	**Measurement (Bq/m^3)**	**Analytical Solution (Bq/m^3)**	**Numerical Simulation (Bq/m^3)**
0.5	16.80	16.78	17.97

The close agreement between measured data, analytical results, and numerical simulations (less than 2% difference) validates the accuracy and reliability of the CFD model used in this study. This demonstrates that the simulation can effectively replicate real-world conditions and provides a valuable tool for understanding radon behavior under varying environmental factors.

Chapter 5 Conclusions and Recommendations

This study explored the Computational Fluid Dynamics study on the influence of indoor radon in Canadian residential setting. The findings reveal several key insights that contribute to a deeper understanding of radon behaviour in indoor environments.

5.1 Influence of Air Physical Parameters on Radon Concentration

The results indicate that indoor temperature significantly affects radon accumulation. At elevated temperatures (21°C,24°C), radon concentration increased due to the stack effect, which promotes the movement of radon gas from the ground into indoor spaces. Conversely, at a moderate temperature of 18 °C, radon levels were lower, suggesting that maintaining an indoor temperature within this range is effective in minimizing radon exposure, but it also affects other environmental factors. This aligns with previous studies, reinforcing the notion that temperature regulation is a critical factor in radon mitigation.

The study demonstrated that higher humidity levels (60%) tend to reduce radon concentration, as moisture acts as a barrier to radon diffusion. At lower humidity (20%), radon was more freely diffused, leading to higher concentrations. These findings emphasize the importance of maintaining adequate indoor humidity to manage radon levels effectively, as increased humidity facilitates the attachment of radon progeny to particles, reducing airborne radon exposure.

The validation of the CFD model against experimental data confirmed its accuracy and reliability, making it a valuable tool for analyzing indoor radon distribution. The ability to simulate complex interactions between radon and environmental factors offers a cost-effective and flexible method for studying indoor air quality, which can be applied to various building types and scenarios.

5.2 Limitations of the Study

1. **Limited Seasonal Analysis**: This study was conducted primarily during the winter heating season, which may not represent radon behavior throughout the year. Radon concentrations

can vary significantly with seasonal changes, and the study's findings might differ in warmer seasons when ventilation patterns and outdoor temperatures change.

2. **Single Case Study**: The research focused on a single-family residential house in Victoria, BC, with specific construction characteristics and environmental conditions. As a result, the findings may not be directly applicable to other building types, regions, or climates with different architectural designs and radon entry pathways.

3. **Simplified CFD Model Assumptions**: While the CFD simulations provided valuable insights, certain assumptions, such as steady-state conditions, simplified geometry, and idealized boundary conditions, might not fully capture the complexities of real-world indoor environments. These simplifications may limit the accuracy of predicting radon behavior in more dynamic or complex indoor settings.

4. **Limited Environmental Factors**: The study primarily focused on the influence of temperature, humidity, and ventilation rates on radon concentrations. Other factors, such as building materials, soil characteristics, wind speed, and pressure differences, which can also affect indoor radon levels, were not thoroughly investigated.

5. **Measurement Equipment Accuracy**: The accuracy of radon measurements relies on the sensitivity and calibration of the detectors used. While continuous radon monitors provided real-time data, slight inaccuracies or calibration issues could affect the precision of the recorded radon concentrations.

6. **Short-Term Monitoring Period**: The radon measurements in this study were conducted over a relatively short monitoring period of six weeks. While this duration provided valuable insights into radon behavior, it may not fully capture long-term trends or seasonal fluctuations that occur over a year. Furthermore, the use of only one detector limited the scope of the data to point to concentration values, potentially overlooking spatial variations in radon accumulation within the building. To gain a more comprehensive understanding of radon behavior under varying environmental conditions, multiple detectors should be deployed across different locations within the building for a longer monitoring period. This approach would enhance the reliability of the findings and provide a more holistic view of radon distribution patterns.

7. **Influence of Occupant Behavior**: The study did not account for the impact of occupant activities, such as window opening, HVAC usage, or changes in furniture layout, which can influence radon distribution and concentrations in real-world settings. These factors can introduce variability that may not be captured in the controlled study environment.
8. **Limited Scope of Radon Mitigation Techniques**: The study primarily analyzed radon behavior under different environmental conditions but did not extensively evaluate the effectiveness of various radon mitigation strategies. Further investigation into how different mitigation methods impact radon concentrations would provide more practical recommendations.

5.3 Future Works

The study focused on radon measurements during the winter heating season, which is typically when radon levels are highest due to reduced ventilation. However, future research should include long-term monitoring across different seasons to capture the variations in radon concentrations and the effects of changing outdoor environmental factors such as temperature, wind speed, and humidity.

Future research should explore more complex CFD simulations that incorporate different building layouts, construction materials, and ventilation strategies to understand how these factors affect radon behavior in various indoor settings. Investigating the impact of building envelope tightness, multi-story structures, and the presence of HVAC systems will provide a more comprehensive understanding of radon distribution in diverse environments.

Further research is needed to evaluate the effectiveness of various radon mitigation techniques, such as sub-slab depressurization, active ventilation systems, and the use of radon barriers in different building types. By integrating CFD simulations with experimental data, researchers can assess the efficiency of these methods under varying conditions, providing recommendations for the most effective solutions in reducing indoor radon levels.

Considering the growing emphasis on energy efficiency, future studies should investigate the relationship between radon mitigation strategies and building energy performance. Research can

explore how different ventilation rates, insulation levels, and HVAC system configurations affect both radon concentration and energy consumption, aiming to develop integrated solutions that optimize indoor air quality without compromising energy efficiency.

The impact of occupant behavior on radon exposure, such as opening windows, using fans, or adjusting thermostats, to better understand how these actions influence radon distribution and concentration. This approach will provide more practical insights into how daily habits can affect indoor air quality and help develop personalized mitigation strategies.

Advancements in real-time radon detection and smart monitoring technologies offer opportunities for more accurate and continuous indoor radon assessments. Future research can explore integrating these technologies with CFD modeling to create dynamic models that respond to changing indoor conditions, providing more effective and responsive radon management strategies.

Future CFD studies should explore the use of finer meshing techniques and adaptive meshing to enhance the resolution of radon dispersion simulations. This is especially important near critical areas such as cracks in building envelopes, joints between materials, or foundation seams where radon ingress is more significant. Improved resolution can provide more accurate data on radon concentration gradients and aid in designing targeted mitigation strategies.

Conducting collaborative studies that combine CFD simulations with large-scale experimental radon testing is essential. Experimental validation using controlled setups and real-world buildings across diverse environmental and architectural conditions can ensure the robustness of simulation findings. These validations will bridge the gap between theoretical predictions and practical applications, improving confidence in CFD as a tool for radon research. Expanding CFD models to simulate radon behavior in the presence of other indoor pollutants, such as carbon dioxide, volatile organic compounds (VOCs), and particulate matter, can provide a more comprehensive understanding of indoor air quality dynamics. These advanced models should include pollutant interactions, transport mechanisms, and the influence of ventilation systems to develop holistic indoor air quality management strategies.

There is a need for further research into how the findings from this study can inform public policy and building codes related to radon mitigation. Additionally, exploring strategies to increase public awareness about radon risks, testing, and mitigation can contribute to a more informed and proactive approach to indoor air quality management.

References

1. Charles, M. (2010). Effects of Ionizing Radiation: United Nations Scientific Committee on the Effects of Atomic Radiation: UNSCEAR 2006 Report, Volume 1—Report to the General Assembly, with Scientific Annexes A and B. *Radiation Protection Dosimetry*, *138*(2), 187–189.
2. Organization, W. Health. (2009). *WHO Handbook on Indoor Radon : a Public Health Perspective*. World Health Organization.
3. Grzywa-Celińska, A., Krusiński, A., Mazur, J., Szewczyk, K., & Kozak, K. (2020). Radon—the element of risk. The impact of radon exposure on human health. *Toxics*, *8*(4), 1–20. https://doi.org/10.3390/toxics8040120
4. Field, R. W. (2011). Radon: An Overview of Health Effects. In Encyclopedia of Environmental Health, Volume 1-5 (Vol. 4, pp. V4-745-V4-753). Elsevier. https://doi.org/10.1016/B978-0-444-52272-6.00095-7
5. Degu Belete, G., & Alemu Anteneh, Y. (2021). General Overview of Radon Studies in Health Hazard Perspectives. In *Journal of Oncology* (Vol. 2021). https://doi.org/10.1155/2021/6659795
6. Robertson, A., Allen, J., Laney, R., & Curnow, A. (2013). The cellular and molecular carcinogenic effects of radon exposure: A review. In *International Journal of Molecular Sciences* (Vol. 14, Issue 7, pp. 14024–14063). https://doi.org/10.3390/ijms140714024
7. Chen, J., Moir, D., & Whyte, J. (2012). Canadian population risk of radon induced lung cancer: A re-assessment based on the recent cross-Canada radon survey. *Radiation Protection Dosimetry*, *152*(1–3). https://doi.org/10.1093/rpd/ncs147
8. Ishimori, Y., Lange, K., Martin, P., Mayya, Y. S., & Phaneuf, M. (n.d.). Measurement and Calculation of Radon Releases from NORM Residues.
9. Nunes, L. J. R., Curado, A., da Graça, L. C. C., Soares, S., & Lopes, S. I. (2022). Impacts of Indoor Radon on Health: A Comprehensive Review on Causes, Assessment and Remediation Strategies. In *International Journal of Environmental Research and Public Health* (Vol. 19, Issue 7). https://doi.org/10.3390/ijerph19073929
10. Altendorf, D., Wienkenjohann, H., Berger, F., Dehnert, J., Grünewald, H., Naumov, D., Trabitzsch, R., & Weiß, H. (2024). Successful reduction of indoor radon activity

concentration via cross-ventilation: experimental data and CFD simulations. *Isotopes in Environmental and Health Studies*, *60*(1). https://doi.org/10.1080/10256016.2023.2282686

11. Health Canada. (2009, November 24). Radon guideline. Canada.ca. https://www.canada.ca/en/health-canada/services/health-risks-safety/radiation/radon/government-canada-radon-guideline.html
12. Akbari, K., Mahmoudi, J., & Ghanbari, M. (2013). Influence of indoor air conditions on radon concentration in a detached house. *Journal of Environmental Radioactivity*, *116*, 166–173. https://doi.org/10.1016/j.jenvrad.2012.08.013
13. Chauhan, N., Chauhan, R. P., Joshi, M., Agarwal, T. K., Aggarwal, P., & Sahoo, B. K. (2014). Study of indoor radon distribution using measurements and CFD modeling. *Journal of Environmental Radioactivity*, *136*, 105–111. https://doi.org/10.1016/j.jenvrad.2014.05.020
14. Adelikhah, M., Imani, M., & Kovács, T. (2023). Measurements and computational fluid dynamics investigation of the indoor radon distribution in a typical naturally ventilated room. *Scientific Reports*, *13*(1). https://doi.org/10.1038/s41598-022-23642-7
15. Rabi, R., & Oufni, L. (2017). Study of radon dispersion in typical dwelling using CFD modeling combined with passive-active measurements. In *Radiation Physics and Chemistry* (Vol. 139, pp. 40–48). Elsevier Ltd. https://doi.org/10.1016/j.radphyschem.2017.04.012
16. Moore, J., & Lavoie Katherine Guindon-Kezis, F. (2022). *Health Canada's Indoor Air Program: Risk Assessment and Research to Support Standards Development*. www.ashrae.org
17. Health Canada, (2018). *House Dust Mites in the Residential Indoor Environment | Technical Document Ventilation and the Indoor Environment Picture/artwork area*.
18. William, L. R. (1990). Toxicological profile for radon. New York: U.S. Public Health Service, in collaboration with U.S. Environmental Protection Agency. Retrieved 12.4.2010, from http://www.bvsde.paho.org/bvstox/i/fulltext/ toxprofiles/radon.pdf
19. Phong Thu, H. N., van Thang, N., & Hao, L. C. (2020). The effects of some soil characteristics on radon emanation and diffusion. *Journal of Environmental Radioactivity*, *216*. https://doi.org/10.1016/j.jenvrad.2020.106189

20. Nazaroff, W. W., Feustel, H., Nero, A. v., Revzan, K. L., Grimsrud, D. T., Essling, M. A., & Toohey, R. E. (1985). Radon transport into a detached one-story house with a basement. Atmospheric Environment (1967), 19(1). https://doi.org/10.1016/0004-6981(85)90134-9
21. Epa, U., & Environments Division, I. (1991). *Indoor Air Facts No. 4 Sick Building Syndrome*.
22. Chen, J., Moir, D., & Whyte, J. (2012). Canadian population risk of radon induced lung cancer: A re-assessment based on the recent cross-Canada radon survey. *Radiation Protection Dosimetry*, *152*(1–3), 9–13. https://doi.org/10.1093/rpd/ncs147
23. Khan, S. M., Pearson, D. D., Rönnqvist, T., Nielsen, M. E., Taron, J. M., & Goodarzi, A. A. (2021). Rising Canadian and falling Swedish radon gas exposure as a consequence of 20th to 21st century residential build practices. *Scientific Reports*, *11*(1). https://doi.org/10.1038/s41598-021-96928-x
24. Stanley, F. K. T., Zarezadeh, S., Dumais, C. D., Dumais, K., MacQueen, R., Clement, F., & Goodarzi, A. A. (2017). Comprehensive survey of household radon gas levels and risk factors in southern Alberta. *CMAJ Open*, *5*(1). https://doi.org/10.9778/cmajo.20160142
25. Whyte, J., Falcomer, R., & Chen, J. (2019). A Comparative Study of Radon Levels in Federal Buildings and Residential Homes in Canada. *Health Physics*, *117*(3). https://doi.org/10.1097/HP.0000000000001057
26. Sonntag D. 1990. Important new values of the physical constants of 1986, vapor pressure formulations based on ITS-90 and psychrometer formulae. Zeitschrift für Meteorologie 40:340-344.
27. Ansys Fluent 12.0 theory guide - 7.1.1 species transport equations. (n.d.). https://www.afs.enea.it/project/neptunius/docs/fluent/html/th/node128.htm#lewis-number-def
28. Anderson, J. D., & Anderson Jr, J. D. (1995). Computational Fluid Dynamics The Basics with Applications. In *McGrawhill Inc*.
29. Chakraverty, S., Sahoo, B. K., Rao, T. D., Karunakar, P., & Sapra, B. K. (2018). Modelling uncertainties in the diffusion-advection equation for radon transport in soil using interval arithmetic. *Journal of Environmental Radioactivity*, *182*, 165–171. https://doi.org/10.1016/j.jenvrad.2017.12.007

30. Chauhan, N. (2023). Investigation of Radon Gas Diffusion through Thermocol Sheet: Effect of Thickness. *Indian Journal of Pure and Applied Physics*, *61*(6), 472–477. https://doi.org/10.56042/ijpap.v61i6.2422
31. Ashrae. (2007). *Hygrothermal Properties of Exterior Claddings, Sheathing Boards, Membranes, and Insulation Materials for Building Envelope Design*.
32. Elshafei, G., Negm, A., Bady, M., Suzuki, M., & Ibrahim, M. G. (2017). Numerical and experimental investigations of the impacts of window parameters on indoor natural ventilation in a residential building. *Energy and Buildings*, *141*, 321–332. https://doi.org/10.1016/j.enbuild.2017.02.055
33. General, C., & Board, S. (n.d.). *Government of Canada Canadian General Standards Board Gouvernement du Canada Office des normes générales du Canada Expérience et excellence Experience and excellence Radon control options for new buildings*. www.scc.ca.
34. Harrje, D. T., Hubbard, L. M., Gadsby, K. J., Bolker, B., & Bohac, D. L. (1989). The effect of radon mitigation systems on ventilation in buildings. *ASHRAE TRANS.: TECHNICAL AND SYMP. PAPERS PRESENTED AT THE 1989 WINTER MEET., CHICAGO, U.S.A., ATLANTA, U.S.A., ASHRAE INC.*, *95*(1, 1989, pp.107-113. (3210)).
35. ASHRAE (2016a) "Standard 62.1. Ventilation for Acceptable Indoor Air Quality." American Society of Heating, Refrigerating and Air-Conditioning Engineers.
36. ASHRAE (2016b) "Standard 62.2. Ventilation and Acceptable Indoor Air Quality in Low-Rise Residential Buildings." American Society of Heating, Refrigerating and Air-Conditioning Engineers.
37. CAN/CSA (2014) "F326 M91. Residential Mechanical Ventilation Systems." Canadian Standards Association.
38. Meyer, W. (2019). Impact of constructional energy-saving measures on radon levels indoors. *Indoor Air*, *29*(4). https://doi.org/10.1111/ina.12553
39. Parkash, R., Chauhan, N., & Chauhan, R. P. (2024). Application of CFD modeling for indoor radon and thoron dispersion study: A review. In *Journal of Environmental Radioactivity* (Vol. 272). Elsevier Ltd. https://doi.org/10.1016/j.jenvrad.2023.107368
40. Prasad, Y., Prasad, G., Gusain, G. S., Choubey, V. M., & Ramola, R. C. (2009). Seasonal variation on radon emission from soil and water. In *Indian J. Phys* (Vol. 83, Issue 7).

41. Radon in the human environment: Assessing the picture. (1994). In IAEA BULLETIN [Journal-article].https://www.iaea.org/sites/default/files/publications/magazines/bulletin/bull36/36205643235.pdf
42. Spasić, D., & Gulan, L. (2022). High Indoor Radon Case Study: Influence of Meteorological Parameters and Indication of Radon Prone Area. *Atmosphere*, *13*(12). https://doi.org/10.3390/atmos13122120
43. Symonds, P., Rees, D., Daraktchieva, Z., McColl, N., Bradley, J., Hamilton, I., & Davies, M. (2019). Home energy efficiency and radon: An observational study. *Indoor Air*, *29*(5). https://doi.org/10.1111/ina.12575
44. William, L. R. (1990). Toxicological profile for radon. New York: U.S. Public Health Service, in collaboration with U.S. Environmental Protection Agency. Retrieved 12.4.2010, from http://www.bvsde.paho.org/bvstox/i/fulltext/ toxprofiles/radon.pdf
45. Kenway, G. K. W., Mader, C. A., He, P., & Martins, J. R. R. A. (2019). Effective adjoint approaches for computational fluid dynamics. In *Progress in Aerospace Sciences* (Vol. 110). https://doi.org/10.1016/j.paerosci.2019.05.002
46. ANSYS Inc. (2024). ANSYS FLUENT R2 Theory Guide. Canonsburg: ANSYS Inc.

Appendix 1

Table A.1: Weekly Radon Concentration, Temperature, and Humidity Readings

Time	Temperature ℃	Humidity	Dew point ℃	VPD	Radon
2023-11-09 19:00	20.9	0.455	8.7	1.35kPa	34
2023-11-09 20:00	19.9	0.462	8	1.25kPa	15
2023-11-09 21:00	19.7	0.461	7.8	1.24kPa	15
2023-11-09 22:00	19.5	0.46	7.6	1.22kPa	15
2023-11-09 23:00	19.3	0.459	7.4	1.21kPa	19
2023-11-10 0:00	19.8	0.487	8.7	1.18kPa	22
2023-11-10 1:00	20.4	0.491	9.4	1.22kPa	22
2023-11-10 2:00	20.5	0.472	8.9	1.27kPa	21
2023-11-10 3:00	20.1	0.466	8.3	1.26kPa	21
2023-11-10 4:00	19.8	0.465	8	1.24kPa	15
2023-11-10 5:00	19.6	0.463	7.8	1.22kPa	14
2023-11-10 6:00	19.5	0.462	7.6	1.22kPa	15
2023-11-10 7:00	19.3	0.461	7.4	1.21kPa	24
2023-11-10 8:00	19.2	0.465	7.5	1.19kPa	22
2023-11-10 9:00	19.9	0.491	8.9	1.18kPa	22
2023-11-10 10:00	20.4	0.491	9.4	1.22kPa	14
2023-11-10 11:00	20.3	0.464	8.4	1.28kPa	10
2023-11-10 12:00	20.3	0.474	8.7	1.25kPa	27
2023-11-10 13:00	20.3	0.461	8.3	1.28kPa	24
2023-11-10 15:00	20.1	0.458	8	1.28kPa	22
2023-11-10 16:00	19.9	0.458	7.9	1.26kPa	15
2023-11-10 17:00	19.8	0.465	8	1.24kPa	17
2023-11-10 18:00	19.8	0.462	7.9	1.24kPa	15
2023-11-10 19:00	19.6	0.461	7.7	1.23kPa	36
2023-11-10 20:00	19.6	0.466	7.8	1.22kPa	33
2023-11-10 21:00	19.6	0.464	7.8	1.22kPa	22
2023-11-10 22:00	19.7	0.471	8.1	1.21kPa	17
2023-11-10 23:00	19.9	0.464	8.1	1.25kPa	19
2023-11-11 0:00	19.9	0.468	8.2	1.24kPa	15
2023-11-11 1:00	20.4	0.488	9.3	1.23kPa	17
2023-11-11 2:00	20.6	0.475	9	1.27kPa	19
2023-11-11 3:00	20.6	0.468	8.8	1.29kPa	15
2023-11-11 4:00	20.6	0.465	8.7	1.30kPa	14
2023-11-11 5:00	20.5	0.462	8.5	1.30kPa	10
2023-11-11 6:00	20.3	0.461	8.3	1.28kPa	14
2023-11-11 7:00	20.1	0.462	8.2	1.27kPa	19
2023-11-11 8:00	19.8	0.463	7.9	1.24kPa	19
2023-11-11 9:00	19.8	0.465	8	1.24kPa	22
2023-11-11 10:00	19.7	0.464	7.9	1.23kPa	29
2023-11-11 11:00	19.6	0.463	7.8	1.22kPa	15
2023-11-11 12:00	19.6	0.467	7.9	1.22kPa	19
2023-11-11 13:00	19.8	0.463	7.9	1.24kPa	15
2023-11-11 14:00	19.9	0.46	7.9	1.25kPa	29
2023-11-11 15:00	19.9	0.46	7.9	1.25kPa	12
2023-11-11 16:00	19.9	0.471	8.3	1.23kPa	12
2023-11-11 17:00	20	0.466	8.2	1.25kPa	10
2023-11-11 18:00	19.7	0.465	7.9	1.23kPa	10
2023-11-11 19:00	19.6	0.465	7.8	1.22kPa	19
2023-11-11 20:00	19.6	0.472	8	1.20kPa	17
2023-11-11 21:00	19.8	0.461	7.9	1.24kPa	19
2023-11-11 22:00	19.9	0.457	7.8	1.26kPa	10
2023-11-11 23:00	19.9	0.461	8	1.25kPa	14
2023-11-12 0:00	20.3	0.483	9	1.23kPa	12
2023-11-12 1:00	20.2	0.471	8.6	1.25kPa	27
2023-11-12 2:00	20	0.466	8.2	1.25kPa	27
2023-11-12 3:00	19.7	0.464	7.9	1.23kPa	19
2023-11-12 4:00	19.5	0.464	7.7	1.22kPa	22
2023-11-12 5:00	19.3	0.463	7.5	1.20kPa	24

023-11-12 6:00	19.1	0.463	7.3	1.19kPa	19
2023-11-12 7:00	19.1	0.463	7.3	1.19kPa	19
2023-11-12 8:00	19	0.469	7.4	1.17kPa	15
2023-11-12 9:00	19	0.465	7.3	1.18kPa	26
2023-11-12 10:00	19	0.462	7.2	1.18kPa	19
2023-11-12 11:00	18.9	0.461	7.1	1.18kPa	8
2023-11-12 12:00	18.9	0.465	7.2	1.17kPa	33
2023-11-12 13:00	18.9	0.463	7.1	1.17kPa	8
2023-11-12 14:00	18.9	0.47	7.3	1.16kPa	24
2023-11-12 15:00	19.4	0.465	7.6	1.21kPa	17
2023-11-12 16:00	19.5	0.463	7.7	1.22kPa	22
2023-11-12 17:00	19.6	0.459	7.6	1.23kPa	19
2023-11-12 18:00	19.7	0.457	7.7	1.25kPa	14
2023-11-12 19:00	19.8	0.455	7.7	1.26kPa	14
2023-11-12 20:00	19.9	0.454	7.7	1.27kPa	17
2023-11-12 21:00	19.9	0.453	7.7	1.27kPa	19
2023-11-12 22:00	20.1	0.452	7.9	1.29kPa	22
2023-11-12 23:00	20.1	0.451	7.8	1.29kPa	27
2023-11-13 0:00	20.1	0.45	7.8	1.29kPa	15
2023-11-13 1:00	20.1	0.45	7.8	1.29kPa	8
2023-11-13 2:00	20.2	0.449	7.8	1.30kPa	24
2023-11-13 3:00	20.1	0.448	7.7	1.30kPa	22
2023-11-13 4:00	20.1	0.448	7.7	1.30kPa	19
2023-11-13 5:00	20.1	0.447	7.7	1.30kPa	33
2023-11-13 6:00	20	0.447	7.6	1.29kPa	22
2023-11-13 7:00	19.9	0.446	7.5	1.29kPa	15
2023-11-13 8:00	19.8	0.444	7.3	1.28kPa	12
2023-11-13 9:00	19.8	0.444	7.3	1.28kPa	12
2023-11-13 10:00	19.8	0.442	7.3	1.29kPa	22
2023-11-13 11:00	19.8	0.441	7.2	1.29kPa	22
2023-11-13 12:00	19.9	0.441	7.3	1.30kPa	17
2023-11-13 13:00	19.9	0.44	7.3	1.30kPa	19
2023-11-13 14:00	20.1	0.439	7.4	1.32kPa	33
2023-11-13 15:00	20.2	0.437	7.5	1.33kPa	27
2023-11-13 16:00	20.3	0.436	7.5	1.34kPa	26
2023-11-13 17:00	20.4	0.436	7.6	1.35kPa	22
2023-11-13 18:00	20.4	0.435	7.6	1.35kPa	22
2023-11-13 19:00	20.4	0.435	7.6	1.35kPa	34
2023-11-13 20:00	20.4	0.434	7.5	1.36kPa	15
2023-11-13 21:00	20.4	0.433	7.5	1.36kPa	22
2023-11-13 22:00	20.3	0.432	7.4	1.35kPa	29
2023-11-13 23:00	20.3	0.431	7.3	1.36kPa	33
2023-11-14 0:00	20.2	0.43	7.2	1.35kPa	26
2023-11-14 1:00	20.1	0.429	7.1	1.34kPa	26
2023-11-14 2:00	20.1	0.429	7.1	1.34kPa	19
2023-11-14 3:00	19.9	0.427	6.8	1.33kPa	12
2023-11-14 4:00	19.8	0.425	6.7	1.33kPa	17
2023-11-14 5:00	19.6	0.423	6.4	1.32kPa	21
2023-11-14 6:00	19.6	0.423	6.4	1.32kPa	10
2023-11-14 7:00	19.5	0.422	6.3	1.31kPa	27
2023-11-14 8:00	19.4	0.421	6.2	1.30kPa	17
2023-11-14 9:00	19.3	0.421	6.1	1.30kPa	24
2023-11-14 10:00	19.3	0.419	6	1.30kPa	8
2023-11-14 11:00	19.4	0.418	6.1	1.31kPa	15
2023-11-14 12:00	19.4	0.418	6.1	1.31kPa	12
2023-11-14 13:00	19.4	0.418	6.1	1.31kPa	17
2023-11-14 14:00	19.5	0.418	6.2	1.32kPa	8
2023-11-14 15:00	19.5	0.417	6.1	1.32kPa	14
2023-11-14 16:00	19.5	0.417	6.1	1.32kPa	7
2023-11-14 17:00	19.6	0.417	6.2	1.33kPa	17
2023-11-14 18:00	19.6	0.417	6.2	1.33kPa	15
2023-11-14 19:00	19.6	0.417	6.2	1.33kPa	31
2023-11-14 20:00	19.6	0.417	6.2	1.33kPa	27
2023-11-14 21:00	19.5	0.417	6.1	1.32kPa	19
2023-11-14 22:00	19.5	0.417	6.1	1.32kPa	24
2023-11-14 23:00	19.4	0.415	6	1.32kPa	40

2023-11-15 0:00	19.3	0.415	5.9	1.31kPa	40
2023-11-15 1:00	19.3	0.415	5.9	1.31kPa	19
2023-11-15 2:00	19.2	0.414	5.8	1.30kPa	15
2023-11-15 3:00	19.1	0.413	5.6	1.30kPa	19
2023-11-15 4:00	19.1	0.413	5.6	1.30kPa	21
2023-11-15 5:00	19.1	0.413	5.6	1.30kPa	14
2023-11-15 6:00	19	0.412	5.5	1.29kPa	12
2023-11-15 7:00	19	0.412	5.5	1.29kPa	17
2023-11-15 8:00	18.9	0.412	5.4	1.28kPa	26
2023-11-15 9:00	18.9	0.412	5.4	1.28kPa	21
2023-11-15 10:00	18.9	0.412	5.4	1.28kPa	14
2023-11-15 11:00	18.9	0.412	5.4	1.28kPa	14
2023-11-15 12:00	18.9	0.411	5.4	1.29kPa	21
2023-11-15 13:00	18.9	0.411	5.4	1.29kPa	21
2023-11-15 14:00	18.9	0.411	5.4	1.29kPa	14
2023-11-15 15:00	19	0.411	5.5	1.29kPa	15
2023-11-15 16:00	19	0.411	5.5	1.29kPa	19
2023-11-15 17:00	19	0.412	5.5	1.29kPa	12
2023-11-15 18:00	19	0.412	5.5	1.29kPa	12
2023-11-15 19:00	19	0.412	5.5	1.29kPa	14
2023-11-15 21:00	19	0.412	5.5	1.29kPa	52
2023-11-16 0:00	18.8	0.409	5.2	1.28kPa	33
2023-11-16 1:00	18.8	0.409	5.2	1.28kPa	29
2023-11-16 2:00	18.8	0.409	5.2	1.28kPa	12
2023-11-16 3:00	18.7	0.408	5.1	1.28kPa	24
2023-11-16 4:00	18.7	0.408	5.1	1.28kPa	21
2023-11-16 5:00	18.6	0.408	5	1.27kPa	17
2023-11-16 6:00	18.6	0.407	5	1.27kPa	21
2023-11-16 7:00	18.5	0.407	4.9	1.26kPa	29
2023-11-16 8:00	18.5	0.406	4.9	1.27kPa	24
2023-11-16 9:00	18.4	0.404	4.7	1.26kPa	27
2023-11-16 10:00	18.4	0.403	4.7	1.26kPa	31
2023-11-16 11:00	18.4	0.403	4.7	1.26kPa	14
2023-11-16 12:00	18.4	0.401	4.6	1.27kPa	10
2023-11-16 13:00	18.5	0.4	4.6	1.28kPa	14
2023-11-16 14:00	18.6	0.399	4.7	1.29kPa	7
2023-11-16 15:00	18.7	0.399	4.8	1.30kPa	7
2023-11-16 16:00	18.8	0.399	4.9	1.30kPa	8
2023-11-16 17:00	18.8	0.399	4.9	1.30kPa	10
2023-11-16 18:00	18.9	0.408	5.3	1.29kPa	10
2023-11-16 19:00	18.9	0.406	5.2	1.30kPa	19
2023-11-16 20:00	19.1	0.418	5.8	1.29kPa	15
2023-11-16 21:00	19.1	0.411	5.6	1.30kPa	21
2023-11-16 22:00	19.1	0.408	5.5	1.31kPa	41
2023-11-16 23:00	19.1	0.419	5.8	1.28kPa	10
2023-11-17 0:00	19.4	0.433	6.6	1.28kPa	21
2023-11-17 1:00	19.6	0.429	6.6	1.30kPa	15
2023-11-17 2:00	19.2	0.419	5.9	1.29kPa	10
2023-11-17 3:00	18.8	0.415	5.4	1.27kPa	15
2023-11-17 4:00	18.6	0.413	5.2	1.26kPa	10
2023-11-17 5:00	18.4	0.412	5	1.24kPa	24
2023-11-17 6:00	18.1	0.411	4.7	1.22kPa	34
2023-11-17 7:00	18	0.41	4.5	1.22kPa	24
2023-11-17 8:00	17.8	0.41	4.4	1.20kPa	8
2023-11-17 9:00	18.4	0.435	5.8	1.20kPa	7
2023-11-17 10:00	18.9	0.419	5.7	1.27kPa	45
2023-11-17 11:00	19.3	0.407	5.6	1.33kPa	14
2023-11-17 12:00	19.5	0.403	5.6	1.35kPa	22
2023-11-17 13:00	19.7	0.404	5.9	1.37kPa	22
2023-11-17 14:00	20	0.399	5.9	1.41kPa	31
2023-11-17 15:00	20.2	0.398	6.1	1.43kPa	45
2023-11-17 16:00	20.3	0.394	6	1.44kPa	17
2023-11-17 17:00	20.3	0.393	6	1.45kPa	22
2023-11-17 18:00	20.3	0.394	6	1.44kPa	15
2023-11-17 19:00	20.3	0.392	6	1.45kPa	34
2023-11-17 20:00	20.4	0.402	6.4	1.43kPa	21

2023-11-17 21:00	20.8	0.421	7.4	1.42kPa	7
2023-11-17 22:00	20.8	0.402	6.8	1.47kPa	7
2023-11-17 23:00	21	0.418	7.5	1.45kPa	12
2023-11-18 0:00	21.1	0.407	7.2	1.48kPa	7
2023-11-18 1:00	20.6	0.401	6.6	1.45kPa	8
2023-11-18 2:00	20.4	0.398	6.3	1.44kPa	17
2023-11-18 3:00	20.2	0.398	6.1	1.43kPa	7
2023-11-18 4:00	20.3	0.414	6.8	1.40kPa	10
2023-11-18 5:00	20.6	0.426	7.4	1.39kPa	21
2023-11-18 6:00	20.9	0.423	7.6	1.43kPa	19
2023-11-18 7:00	20.6	0.411	6.9	1.43kPa	22
2023-11-18 8:00	20.1	0.406	6.3	1.40kPa	21
2023-11-18 9:00	20	0.403	6.1	1.40kPa	24
2023-11-18 10:00	19.8	0.401	5.8	1.38kPa	19
2023-11-18 11:00	19.8	0.4	5.8	1.39kPa	22
2023-11-18 12:00	19.8	0.403	5.9	1.38kPa	33
2023-11-18 13:00	19.7	0.402	5.8	1.37kPa	19
2023-11-18 14:00	19.6	0.402	5.7	1.36kPa	19
2023-11-18 15:00	19.5	0.401	5.6	1.36kPa	15
2023-11-18 16:00	19.4	0.401	5.5	1.35kPa	21
2023-11-18 17:00	19.3	0.402	5.4	1.34kPa	14
2023-11-18 18:00	19.3	0.402	5.4	1.34kPa	7
2023-11-18 19:00	19.3	0.403	5.5	1.34kPa	15
2023-11-18 20:00	19.2	0.403	5.4	1.33kPa	26
2023-11-18 21:00	19.1	0.404	5.3	1.32kPa	29
2023-11-18 22:00	19.1	0.404	5.3	1.32kPa	21
2023-11-18 23:00	19.1	0.405	5.4	1.32kPa	17
2023-11-19 0:00	19	0.406	5.3	1.31kPa	22
2023-11-19 1:00	19	0.406	5.3	1.31kPa	26
2023-11-19 2:00	19	0.408	5.4	1.30kPa	19
2023-11-19 3:00	18.9	0.408	5.3	1.29kPa	12
2023-11-19 4:00	18.8	0.409	5.2	1.28kPa	14
2023-11-19 5:00	18.8	0.41	5.3	1.28kPa	12
2023-11-19 6:00	18.8	0.41	5.3	1.28kPa	8
2023-11-19 7:00	18.7	0.411	5.2	1.27kPa	14
2023-11-19 8:00	18.7	0.411	5.2	1.27kPa	12
2023-11-19 9:00	18.6	0.411	5.1	1.26kPa	15
2023-11-19 10:00	18.6	0.411	5.1	1.26kPa	15
2023-11-19 11:00	18.6	0.41	5.1	1.26kPa	15
2023-11-19 12:00	18.6	0.41	5.1	1.26kPa	21
2023-11-19 13:00	18.6	0.41	5.1	1.26kPa	17
2023-11-19 14:00	18.7	0.409	5.1	1.27kPa	19
2023-11-19 15:00	18.8	0.409	5.2	1.28kPa	24
2023-11-19 16:00	18.8	0.408	5.2	1.28kPa	17
2023-11-19 17:00	18.8	0.408	5.2	1.28kPa	21
2023-11-19 18:00	18.8	0.408	5.2	1.28kPa	22
2023-11-19 19:00	18.8	0.408	5.2	1.28kPa	19
2023-11-19 20:00	18.8	0.407	5.2	1.29kPa	40
2023-11-19 21:00	18.8	0.416	5.5	1.27kPa	26
2023-11-19 22:00	18.9	0.412	5.4	1.28kPa	33
2023-11-19 23:00	19.2	0.423	6.1	1.28kPa	36
2023-11-20 0:00	19.9	0.436	7.1	1.31kPa	17
2023-11-20 1:00	19.9	0.421	6.6	1.35kPa	27
2023-11-20 2:00	19.8	0.415	6.3	1.35kPa	17
2023-11-20 3:00	19.7	0.413	6.2	1.35kPa	22
2023-11-20 4:00	19.6	0.411	6	1.34kPa	15
2023-11-20 5:00	19.6	0.409	5.9	1.35kPa	12
2023-11-20 6:00	19.5	0.408	5.8	1.34kPa	15
2023-11-20 7:00	19.5	0.408	5.8	1.34kPa	14
2023-11-20 9:00	19.8	0.433	7	1.31kPa	19
2023-11-20 10:00	20.2	0.436	7.4	1.34kPa	22
2023-11-20 11:00	20.4	0.419	7	1.39kPa	15
2023-11-20 12:00	20.5	0.409	6.8	1.43kPa	14
2023-11-20 13:00	20.3	0.406	6.5	1.41kPa	17
2023-11-20 14:00	20.1	0.404	6.2	1.40kPa	14
2023-11-20 15:00	20.1	0.402	6.1	1.41kPa	12

2023-11-20 16:00	20	0.401	6	1.40kPa	8
2023-11-20 17:00	20.1	0.399	6	1.41kPa	12
2023-11-20 18:00	19.9	0.399	5.9	1.40kPa	12
2023-11-20 19:00	19.8	0.399	5.8	1.39kPa	7
2023-11-20 20:00	19.8	0.399	5.8	1.39kPa	14
2023-11-20 21:00	19.8	0.4	5.8	1.39kPa	24
2023-11-20 22:00	19.9	0.395	5.7	1.41kPa	31
2023-11-20 23:00	20.1	0.395	5.9	1.42kPa	29
2023-11-21 0:00	20	0.392	5.7	1.42kPa	24
2023-11-21 1:00	19.8	0.392	5.5	1.40kPa	21
2023-11-21 2:00	19.6	0.392	5.3	1.39kPa	7
2023-11-21 3:00	19.5	0.392	5.2	1.38kPa	31
2023-11-21 4:00	19.5	0.392	5.2	1.38kPa	22
2023-11-21 5:00	19.4	0.392	5.2	1.37kPa	17
2023-11-21 6:00	19.3	0.392	5.1	1.36kPa	14
2023-11-21 7:00	19.3	0.392	5.1	1.36kPa	15
2023-11-21 8:00	19.3	0.392	5.1	1.36kPa	17
2023-11-21 9:00	19.5	0.413	6	1.33kPa	24
2023-11-21 10:00	20	0.425	6.9	1.34kPa	10
2023-11-21 11:00	20.4	0.429	7.4	1.37kPa	8
2023-11-21 12:00	20.5	0.411	6.8	1.42kPa	14
2023-11-21 13:00	20.6	0.406	6.7	1.44kPa	15
2023-11-21 14:00	20.7	0.4	6.6	1.46kPa	10
2023-11-21 15:00	20.6	0.398	6.4	1.46kPa	14
2023-11-21 16:00	20.6	0.397	6.4	1.46kPa	17
2023-11-21 17:00	20.6	0.396	6.4	1.47kPa	22
2023-11-21 18:00	20.7	0.394	6.4	1.48kPa	19
2023-11-21 19:00	20.9	0.394	6.6	1.50kPa	15
2023-11-21 20:00	21.6	0.398	7.3	1.55kPa	8
2023-11-21 21:00	22.1	0.401	7.9	1.59kPa	7
2023-11-21 22:00	22.2	0.393	7.7	1.62kPa	10
2023-11-21 23:00	22.6	0.407	8.6	1.63kPa	10
2023-11-22 0:00	22.8	0.408	8.8	1.64kPa	10
2023-11-22 1:00	22.6	0.4	8.3	1.65kPa	12
2023-11-22 2:00	22.4	0.398	8.1	1.63kPa	22
2023-11-22 3:00	22.2	0.397	7.8	1.61kPa	8
2023-11-22 4:00	22	0.396	7.6	1.60kPa	22
2023-11-22 5:00	22	0.395	7.6	1.60kPa	17
2023-11-22 6:00	22	0.395	7.6	1.60kPa	15
2023-11-22 7:00	21.8	0.394	7.4	1.58kPa	12
2023-11-22 8:00	21.8	0.393	7.3	1.59kPa	19
2023-11-22 9:00	22	0.41	8.1	1.56kPa	24
2023-11-22 10:00	22.4	0.409	8.5	1.60kPa	22
2023-11-22 11:00	22.5	0.397	8.1	1.64kPa	21
2023-11-22 12:00	22.5	0.391	7.9	1.66kPa	17
2023-11-22 13:00	22.5	0.388	7.8	1.67kPa	15
2023-11-22 14:00	22.7	0.385	7.8	1.70kPa	12
2023-11-22 15:00	22.7	0.383	7.8	1.70kPa	15
2023-11-22 16:00	22.6	0.391	8	1.67kPa	8
2023-11-22 17:00	22.7	0.39	8	1.68kPa	8
2023-11-22 18:00	22.6	0.392	8	1.67kPa	14
2023-11-22 19:00	22.7	0.385	7.8	1.70kPa	10
2023-11-22 20:00	22.6	0.383	7.7	1.69kPa	12
2023-11-22 21:00	22.5	0.394	8	1.65kPa	17
2023-11-22 22:00	22.9	0.402	8.6	1.67kPa	12
2023-11-22 23:00	23.2	0.406	9.1	1.69kPa	7
2023-11-23 0:00	23.2	0.383	8.2	1.75kPa	10
2023-11-23 1:00	23.2	0.392	8.5	1.73kPa	7
2023-11-23 2:00	22.8	0.384	7.9	1.71kPa	43
2023-11-23 3:00	22.6	0.38	7.6	1.70kPa	15
2023-11-23 4:00	22.1	0.378	7	1.65kPa	12
2023-11-23 5:00	22.1	0.376	7	1.66kPa	19
2023-11-23 6:00	21.8	0.374	6.6	1.63kPa	12
2023-11-23 7:00	21.7	0.372	6.4	1.63kPa	12
2023-11-23 8:00	21.5	0.371	6.2	1.61kPa	17
2023-11-23 9:00	21.6	0.387	6.9	1.58kPa	17

2023-11-23 10:00	22.1	0.397	7.7	1.60kPa	17
2023-11-23 11:00	22.4	0.383	7.5	1.67kPa	12
2023-11-23 12:00	21.6	0.378	6.6	1.60kPa	14
2023-11-23 13:00	21	0.378	6.1	1.55kPa	8
2023-11-23 14:00	20.8	0.378	5.9	1.53kPa	14
2023-11-23 15:00	20.7	0.381	5.9	1.51kPa	12
2023-11-23 16:00	20.8	0.384	6.1	1.51kPa	10
2023-11-23 17:00	21.2	0.402	7.1	1.51kPa	7
2023-11-23 18:00	21.3	0.393	6.9	1.54kPa	7
2023-11-23 19:00	21.2	0.384	6.5	1.55kPa	15
2023-11-23 20:00	21.1	0.379	6.2	1.55kPa	15
2023-11-23 21:00	21	0.377	6	1.55kPa	8
2023-11-23 22:00	20.8	0.375	5.8	1.54kPa	19
2023-11-23 23:00	20.8	0.374	5.7	1.54kPa	15
2023-11-24 2:00	21.1	0.389	6.6	1.53kPa	21
2023-11-24 3:00	21	0.38	6.1	1.54kPa	12
2023-11-24 4:00	20.5	0.378	5.6	1.50kPa	10
2023-11-24 5:00	20.2	0.374	5.2	1.48kPa	7
2023-11-24 6:00	20.1	0.371	5	1.48kPa	8
2023-11-24 7:00	19.9	0.37	4.8	1.46kPa	7
2023-11-24 8:00	19.7	0.372	4.7	1.44kPa	7
2023-11-24 9:00	20.1	0.397	6	1.42kPa	7
2023-11-24 10:00	20.8	0.398	6.6	1.48kPa	24
2023-11-24 11:00	20.9	0.39	6.4	1.51kPa	15
2023-11-24 12:00	21	0.38	6.1	1.54kPa	12
2023-11-24 13:00	20.9	0.373	5.8	1.55kPa	15
2023-11-24 14:00	20.8	0.369	5.5	1.55kPa	8
2023-11-24 15:00	20.9	0.366	5.5	1.57kPa	17
2023-11-24 16:00	20.9	0.365	5.5	1.57kPa	7
2023-11-24 17:00	20.9	0.371	5.7	1.55kPa	8
2023-11-24 18:00	21.3	0.387	6.7	1.55kPa	12
2023-11-24 19:00	21.2	0.376	6.2	1.57kPa	12
2023-11-24 20:00	21.2	0.368	5.8	1.59kPa	19
2023-11-24 21:00	21.1	0.363	5.6	1.59kPa	12
2023-11-24 22:00	21	0.361	5.4	1.59kPa	10
2023-11-24 23:00	21.1	0.377	6.1	1.56kPa	15
2023-11-25 0:00	21.2	0.385	6.5	1.55kPa	15
2023-11-25 1:00	21.2	0.375	6.1	1.57kPa	22
2023-11-25 2:00	20.8	0.371	5.6	1.55kPa	34
2023-11-25 3:00	20.5	0.369	5.3	1.52kPa	15
2023-11-25 4:00	20.3	0.367	5	1.51kPa	14
2023-11-25 5:00	20.1	0.366	4.8	1.49kPa	14
2023-11-25 6:00	20	0.365	4.7	1.48kPa	14
2023-11-25 7:00	19.8	0.365	4.5	1.47kPa	7
2023-11-25 8:00	19.7	0.364	4.4	1.46kPa	8
2023-11-25 9:00	19.6	0.371	4.5	1.43kPa	7
2023-11-25 10:00	19.9	0.38	5.2	1.44kPa	21
2023-11-25 11:00	20	0.381	5.3	1.45kPa	15
2023-11-25 12:00	20.1	0.369	4.9	1.48kPa	10
2023-11-25 13:00	20.4	0.371	5.3	1.51kPa	7
2023-11-25 14:00	20.6	0.363	5.1	1.55kPa	7
2023-11-25 15:00	20.6	0.363	5.1	1.55kPa	7
2023-11-25 16:00	20.6	0.362	5.1	1.55kPa	7
2023-11-25 17:00	20.6	0.361	5	1.55kPa	15
2023-11-25 18:00	20.6	0.361	5	1.55kPa	14
2023-11-25 19:00	20.4	0.36	4.8	1.53kPa	10
2023-11-25 20:00	20.1	0.36	4.6	1.51kPa	7
2023-11-25 21:00	20	0.361	4.5	1.49kPa	12
2023-11-25 22:00	19.8	0.361	4.3	1.48kPa	10
2023-11-26 0:00	19.6	0.37	4.5	1.44kPa	26
2023-11-26 1:00	19.7	0.369	4.6	1.45kPa	17
2023-11-26 2:00	19.8	0.365	4.5	1.47kPa	17
2023-11-26 3:00	19.8	0.363	4.4	1.47kPa	14
2023-11-26 4:00	19.8	0.362	4.4	1.47kPa	10
2023-11-26 6:00	19.9	0.361	4.4	1.48kPa	10
2023-11-26 7:00	19.9	0.361	4.4	1.48kPa	33

2023-11-26 8:00	19.8	0.361	4.3	1.48kPa	33
2023-11-26 9:00	19.8	0.36	4.3	1.48kPa	24
2023-11-26 10:00	19.8	0.37	4.7	1.45kPa	29
2023-11-26 11:00	20.1	0.37	4.9	1.48kPa	15
2023-11-26 12:00	20.4	0.365	5	1.52kPa	7
2023-11-26 13:00	20.5	0.382	5.8	1.49kPa	12
2023-11-26 14:00	20.8	0.383	6.1	1.52kPa	7
2023-11-26 15:00	21.3	0.394	6.9	1.54kPa	7
2023-11-26 16:00	21.3	0.38	6.4	1.57kPa	7
2023-11-26 17:00	21.1	0.399	6.9	1.50kPa	7
2023-11-26 18:00	21.1	0.383	6.3	1.54kPa	12
2023-11-26 19:00	21.1	0.391	6.6	1.52kPa	7
2023-11-26 20:00	21.1	0.381	6.3	1.55kPa	7
2023-11-26 21:00	21	0.375	5.9	1.55kPa	7
2023-11-26 22:00	20.7	0.373	5.6	1.53kPa	7
2023-11-26 23:00	20.7	0.393	6.4	1.48kPa	7
2023-11-27 0:00	20.7	0.381	5.9	1.51kPa	7
2023-11-27 1:00	20.3	0.379	5.5	1.48kPa	7
2023-11-27 2:00	20	0.376	5.1	1.46kPa	7
2023-11-27 3:00	19.9	0.376	5	1.45kPa	7
2023-11-27 4:00	19.8	0.376	4.9	1.44kPa	7
2023-11-27 5:00	19.6	0.375	4.7	1.43kPa	10
2023-11-27 6:00	19.5	0.375	4.6	1.42kPa	7
2023-11-27 7:00	19.8	0.395	5.6	1.40kPa	10
2023-11-27 8:00	20.1	0.385	5.5	1.45kPa	17
2023-11-27 9:00	20.1	0.394	5.9	1.43kPa	7
2023-11-27 10:00	20.4	0.385	5.8	1.47kPa	12
2023-11-27 11:00	20.5	0.379	5.6	1.50kPa	14
2023-11-27 12:00	20.3	0.374	5.3	1.49kPa	7
2023-11-27 13:00	20.1	0.373	5.1	1.48kPa	7
2023-11-27 14:00	20	0.371	4.9	1.47kPa	8
2023-11-27 15:00	20	0.377	5.1	1.46kPa	17
2023-11-27 16:00	20.2	0.38	5.4	1.47kPa	10
2023-11-27 17:00	20.5	0.373	5.4	1.51kPa	7
2023-11-27 18:00	20.8	0.383	6.1	1.52kPa	7
2023-11-27 19:00	21.1	0.395	6.8	1.51kPa	8
2023-11-27 20:00	21.5	0.395	7.1	1.55kPa	7
2023-11-27 21:00	21.3	0.382	6.5	1.57kPa	7
2023-11-27 22:00	21.3	0.379	6.4	1.57kPa	7
2023-11-27 23:00	21.1	0.375	6	1.56kPa	12
2023-11-28 0:00	20.6	0.374	5.5	1.52kPa	14
2023-11-28 1:00	20.3	0.374	5.3	1.49kPa	7
2023-11-28 2:00	20.1	0.374	5.1	1.47kPa	15
2023-11-28 3:00	20	0.374	5	1.46kPa	10
2023-11-28 4:00	19.8	0.374	4.8	1.45kPa	12
2023-11-28 5:00	19.6	0.373	4.6	1.43kPa	8
2023-11-28 6:00	19.6	0.373	4.6	1.43kPa	17
2023-11-28 7:00	19.5	0.373	4.5	1.42kPa	12
2023-11-28 8:00	19.4	0.375	4.5	1.41kPa	14
2023-11-28 9:00	19.8	0.4	5.8	1.39kPa	12
2023-11-28 10:00	20.1	0.408	6.4	1.39kPa	15
2023-11-28 11:00	20.1	0.397	6	1.42kPa	12
2023-11-28 12:00	20.3	0.39	5.9	1.45kPa	8
2023-11-28 13:00	20.1	0.384	5.5	1.45kPa	8
2023-11-28 14:00	20	0.382	5.3	1.45kPa	19
2023-11-28 15:00	19.9	0.38	5.2	1.44kPa	7
2023-11-28 16:00	19.8	0.378	5	1.44kPa	17
2023-11-28 17:00	19.8	0.379	5	1.43kPa	8
2023-11-28 18:00	20	0.398	5.9	1.41kPa	14
2023-11-28 19:00	20.1	0.384	5.5	1.45kPa	15
2023-11-28 20:00	20.5	0.423	7.2	1.39kPa	24
2023-11-28 21:00	20.9	0.412	7.2	1.45kPa	12
2023-11-28 22:00	20.8	0.394	6.5	1.49kPa	14
2023-11-28 23:00	20.7	0.385	6.1	1.50kPa	14
2023-11-29 0:00	20.8	0.402	6.8	1.47kPa	10
2023-11-29 1:00	20.7	0.385	6.1	1.50kPa	33

2023-11-29 2:00	20.6	0.377	5.7	1.51kPa	19
2023-11-29 3:00	20.4	0.373	5.3	1.50kPa	8
2023-11-29 4:00	20.3	0.371	5.2	1.50kPa	15
2023-11-29 5:00	20.1	0.369	4.9	1.48kPa	21
2023-11-29 6:00	20	0.367	4.7	1.48kPa	21
2023-11-29 7:00	19.8	0.367	4.6	1.46kPa	27
2023-11-29 8:00	19.6	0.367	4.4	1.44kPa	22
2023-11-29 9:00	19.5	0.367	4.3	1.43kPa	22
2023-11-29 10:00	19.4	0.367	4.2	1.43kPa	21
2023-11-29 11:00	19.3	0.366	4.1	1.42kPa	24
2023-11-29 12:00	19.3	0.366	4.1	1.42kPa	17
2023-11-29 13:00	19.3	0.366	4.1	1.42kPa	19
2023-11-29 14:00	19.7	0.387	5.2	1.41kPa	12
2023-11-29 15:00	20.2	0.405	6.3	1.41kPa	26
2023-11-29 16:00	20.8	0.395	6.5	1.49kPa	19
2023-11-29 18:00	21.1	0.389	6.6	1.53kPa	36
2023-11-29 19:00	21.1	0.377	6.1	1.56kPa	21
2023-11-29 20:00	21.1	0.373	6	1.57kPa	14
2023-11-29 21:00	21.1	0.369	5.8	1.58kPa	24
2023-11-29 22:00	21.1	0.366	5.7	1.59kPa	33
2023-11-29 23:00	21.1	0.365	5.6	1.59kPa	26
2023-11-30 0:00	21	0.364	5.5	1.58kPa	26
2023-11-30 1:00	20.7	0.363	5.2	1.56kPa	22
2023-11-30 2:00	20.6	0.363	5.1	1.55kPa	22
2023-11-30 3:00	20.6	0.363	5.1	1.55kPa	17
2023-11-30 4:00	20.4	0.363	4.9	1.53kPa	12
2023-11-30 5:00	20.3	0.362	4.8	1.52kPa	24
2023-11-30 6:00	20.2	0.362	4.7	1.51kPa	17
2023-11-30 7:00	20.1	0.362	4.6	1.50kPa	15
2023-11-30 8:00	20.1	0.366	4.8	1.49kPa	22
2023-11-30 9:00	20.4	0.369	5.2	1.51kPa	27
2023-11-30 10:00	20.6	0.36	5	1.55kPa	17
2023-11-30 11:00	20.6	0.354	4.8	1.57kPa	21
2023-11-30 12:00	20.6	0.353	4.7	1.57kPa	8
2023-11-30 13:00	20.5	0.352	4.6	1.56kPa	15
2023-11-30 14:00	20.4	0.353	4.5	1.55kPa	14
2023-11-30 15:00	20.3	0.353	4.5	1.54kPa	15
2023-11-30 16:00	20.2	0.353	4.4	1.53kPa	27
2023-11-30 17:00	20.1	0.354	4.3	1.52kPa	24
2023-11-30 18:00	20.1	0.357	4.4	1.51kPa	12
2023-11-30 20:00	20.3	0.364	4.9	1.51kPa	10
2023-11-30 21:00	20.4	0.362	4.9	1.53kPa	31
2023-11-30 22:00	20.6	0.358	4.9	1.56kPa	22
2023-11-30 23:00	20.7	0.356	4.9	1.57kPa	29
2023-12-01 0:00	20.9	0.377	5.9	1.54kPa	26
2023-12-01 1:00	21.2	0.373	6	1.58kPa	24
2023-12-01 2:00	21	0.369	5.7	1.57kPa	38
2023-12-01 3:00	20.7	0.367	5.4	1.55kPa	38
2023-12-01 4:00	20.6	0.367	5.3	1.54kPa	38
2023-12-01 5:00	20.6	0.366	5.2	1.54kPa	24
2023-12-01 6:00	20.5	0.366	5.1	1.53kPa	17
2023-12-01 7:00	20.4	0.366	5.1	1.52kPa	24
2023-12-01 8:00	20.3	0.37	5.1	1.50kPa	17
2023-12-01 9:00	20.7	0.398	6.5	1.47kPa	26
2023-12-01 10:00	21.3	0.402	7.2	1.51kPa	15
2023-12-01 11:00	21.3	0.379	6.4	1.57kPa	21
2023-12-01 12:00	21.4	0.373	6.2	1.60kPa	17
2023-12-01 14:00	21.2	0.369	5.9	1.59kPa	19
2023-12-01 15:00	21.1	0.373	6	1.57kPa	22
2023-12-01 16:00	21.2	0.374	6.1	1.58kPa	31
2023-12-01 17:00	21.3	0.37	6	1.60kPa	38
2023-12-01 18:00	21.1	0.369	5.8	1.58kPa	15
2023-12-01 19:00	21	0.369	5.7	1.57kPa	15
2023-12-01 21:00	20.8	0.37	5.6	1.55kPa	24
2023-12-01 22:00	20.8	0.37	5.6	1.55kPa	22
2023-12-01 23:00	20.7	0.37	5.5	1.54kPa	27

2023-12-02 0:00	20.7	0.37	5.5	1.54kPa	15
2023-12-02 1:00	20.6	0.37	5.4	1.53kPa	24
2023-12-02 2:00	20.6	0.37	5.4	1.53kPa	33
2023-12-02 3:00	20.6	0.37	5.4	1.53kPa	34
2023-12-02 4:00	20.5	0.371	5.3	1.52kPa	21
2023-12-02 5:00	20.5	0.371	5.3	1.52kPa	19
2023-12-02 6:00	20.4	0.371	5.3	1.51kPa	22
2023-12-02 7:00	20.3	0.371	5.2	1.50kPa	22
2023-12-02 8:00	20.3	0.371	5.2	1.50kPa	34
2023-12-02 9:00	20.2	0.371	5.1	1.49kPa	22
2023-12-02 10:00	20.2	0.371	5.1	1.49kPa	45
2023-12-02 11:00	20.1	0.37	4.9	1.48kPa	22
2023-12-02 12:00	20.1	0.37	4.9	1.48kPa	14
2023-12-02 13:00	20.2	0.37	5	1.49kPa	15
2023-12-02 14:00	20.3	0.37	5.1	1.50kPa	19
2023-12-02 15:00	20.3	0.37	5.1	1.50kPa	31
2023-12-02 16:00	20.4	0.37	5.2	1.51kPa	19
2023-12-02 17:00	20.3	0.37	5.1	1.50kPa	40
2023-12-02 18:00	20.3	0.37	5.1	1.50kPa	19
2023-12-02 19:00	20.3	0.37	5.1	1.50kPa	22
2023-12-02 20:00	20.3	0.371	5.2	1.50kPa	26
2023-12-02 21:00	20.2	0.371	5.1	1.49kPa	21
2023-12-02 22:00	20.2	0.371	5.1	1.49kPa	27
2023-12-02 23:00	20.1	0.371	5	1.48kPa	17
2023-12-03 0:00	20.1	0.371	5	1.48kPa	26
2023-12-03 1:00	20.1	0.371	5	1.48kPa	26
2023-12-03 2:00	20.1	0.371	5	1.48kPa	27
2023-12-03 3:00	20.1	0.371	5	1.48kPa	22
2023-12-03 4:00	20.1	0.37	4.9	1.48kPa	24
2023-12-03 5:00	20.1	0.37	4.9	1.48kPa	26
2023-12-03 6:00	20.1	0.37	4.9	1.48kPa	12
2023-12-03 7:00	20.1	0.371	5	1.48kPa	10
2023-12-03 8:00	20.1	0.37	4.9	1.48kPa	22
2023-12-03 9:00	20.1	0.37	4.9	1.48kPa	12
2023-12-03 10:00	20.1	0.371	5	1.48kPa	19
2023-12-03 11:00	20.1	0.371	5	1.48kPa	12
2023-12-03 12:00	20.1	0.378	5.3	1.46kPa	12
2023-12-03 13:00	20.3	0.395	6.1	1.44kPa	24
2023-12-03 14:00	20.6	0.385	6	1.49kPa	17
2023-12-03 15:00	20.9	0.383	6.2	1.53kPa	8
2023-12-03 16:00	21.2	0.39	6.7	1.54kPa	17
2023-12-03 17:00	21.2	0.385	6.5	1.55kPa	26
2023-12-03 18:00	21.1	0.403	7.1	1.49kPa	22
2023-12-03 19:00	21.7	0.43	8.6	1.48kPa	17
2023-12-03 20:00	21.9	0.411	8.1	1.55kPa	17
2023-12-03 21:00	21.7	0.401	7.5	1.55kPa	19
2023-12-03 22:00	21.6	0.404	7.6	1.54kPa	22
2023-12-03 23:00	21.7	0.418	8.1	1.51kPa	24
2023-12-04 0:00	22	0.414	8.3	1.55kPa	21
2023-12-04 1:00	21.8	0.405	7.8	1.55kPa	12
2023-12-04 2:00	21.6	0.401	7.4	1.55kPa	21
2023-12-04 3:00	21.3	0.399	7.1	1.52kPa	31
2023-12-04 4:00	21.3	0.398	7.1	1.52kPa	33
2023-12-04 5:00	21.2	0.397	6.9	1.52kPa	19
2023-12-04 6:00	21.1	0.395	6.8	1.51kPa	21
2023-12-04 7:00	21.1	0.394	6.7	1.52kPa	15
2023-12-04 8:00	21	0.394	6.7	1.51kPa	17
2023-12-04 9:00	21.3	0.417	7.8	1.48kPa	10
2023-12-04 10:00	21.7	0.422	8.3	1.50kPa	24
2023-12-04 11:00	21.9	0.424	8.5	1.51kPa	24
2023-12-04 12:00	21.6	0.402	7.5	1.54kPa	21
2023-12-04 13:00	21.3	0.397	7	1.53kPa	17
2023-12-04 14:00	21.1	0.397	6.9	1.51kPa	10
2023-12-04 15:00	21	0.401	6.9	1.49kPa	14
2023-12-04 16:00	21.1	0.399	6.9	1.50kPa	19
2023-12-04 17:00	21.2	0.403	7.2	1.50kPa	22

2023-12-04 18:00	21.2	0.399	7	1.51kPa	22
2023-12-04 19:00	21.1	0.398	6.9	1.51kPa	21
2023-12-04 20:00	21	0.399	6.8	1.49kPa	10
2023-12-04 21:00	20.9	0.418	7.4	1.44kPa	15
2023-12-04 22:00	21.4	0.432	8.4	1.45kPa	26
2023-12-04 23:00	21.8	0.435	8.8	1.48kPa	29
2023-12-05 0:00	22.2	0.446	9.6	1.48kPa	31
2023-12-05 1:00	22.6	0.446	9.9	1.52kPa	26
2023-12-05 2:00	23	0.438	10	1.58kPa	26
2023-12-05 3:00	22.9	0.426	9.5	1.60kPa	83
2023-12-05 4:00	22.7	0.421	9.2	1.60kPa	45
2023-12-05 5:00	22.6	0.418	9	1.60kPa	27
2023-12-05 6:00	22.4	0.417	8.7	1.58kPa	14
2023-12-05 7:00	22.1	0.417	8.5	1.55kPa	21
2023-12-05 8:00	21.9	0.417	8.3	1.53kPa	27
2023-12-07 9:00	19.7	0.433	6.9	1.30kPa	7
2023-12-07 10:00	19.9	0.426	6.8	1.33kPa	7
2023-12-07 11:00	19.9	0.419	6.6	1.35kPa	8
2023-12-14 18:00	21.2	0.418	7.7	1.47kPa	10
2023-12-14 19:00	21.3	0.411	7.5	1.49kPa	21
2023-12-14 20:00	21.1	0.405	7.1	1.49kPa	12
2023-12-14 21:00	20.8	0.41	7.1	1.45kPa	17
2023-12-14 22:00	20.7	0.409	6.9	1.44kPa	10
2023-12-14 23:00	20.8	0.406	6.9	1.46kPa	8
2023-12-15 0:00	21	0.422	7.7	1.44kPa	7
2023-12-15 1:00	21	0.411	7.3	1.46kPa	7
2023-12-15 2:00	20.6	0.407	6.8	1.44kPa	12
2023-12-15 3:00	20.3	0.405	6.4	1.42kPa	7
2023-12-15 4:00	20.1	0.405	6.3	1.40kPa	7
2023-12-15 5:00	20.1	0.405	6.3	1.40kPa	7
2023-12-15 6:00	19.9	0.405	6.1	1.38kPa	8
2023-12-15 7:00	19.8	0.405	6	1.37kPa	21
2023-12-15 8:00	19.6	0.406	5.8	1.35kPa	14
2023-12-15 9:00	19.6	0.406	5.8	1.35kPa	10
2023-12-15 10:00	19.6	0.426	6.5	1.31kPa	10
2023-12-15 11:00	19.9	0.416	6.5	1.36kPa	7
2023-12-15 12:00	20.2	0.425	7	1.36kPa	7
2023-12-15 13:00	20.3	0.418	6.9	1.39kPa	7
2023-12-15 14:00	20.1	0.414	6.6	1.38kPa	7
2023-12-15 15:00	20.1	0.413	6.5	1.38kPa	7
2023-12-15 16:00	20.1	0.412	6.5	1.38kPa	14
2023-12-15 17:00	20	0.412	6.4	1.37kPa	8
2023-12-15 18:00	20.1	0.432	7.2	1.34kPa	8
2023-12-15 19:00	20.5	0.439	7.8	1.35kPa	17
2023-12-15 20:00	20.6	0.426	7.4	1.39kPa	15
2023-12-15 21:00	20.9	0.438	8.1	1.39kPa	12
2023-12-15 22:00	21.2	0.44	8.5	1.41kPa	21
2023-12-16 0:00	21	0.416	7.4	1.45kPa	10
2023-12-16 1:00	20.8	0.411	7.1	1.45kPa	17
2023-12-16 3:00	20.6	0.408	6.8	1.44kPa	10
2023-12-16 4:00	20.5	0.407	6.7	1.43kPa	14
2023-12-16 5:00	20.3	0.405	6.4	1.42kPa	12
2023-12-16 6:00	20.3	0.405	6.4	1.42kPa	8
2023-12-16 7:00	20.1	0.405	6.3	1.40kPa	19
2023-12-16 8:00	20.1	0.405	6.3	1.40kPa	12
2023-12-16 9:00	19.9	0.406	6.1	1.38kPa	19
2023-12-16 11:00	20.4	0.425	7.2	1.38kPa	8
2023-12-16 12:00	20.6	0.439	7.9	1.36kPa	15
2023-12-16 13:00	21.1	0.43	8	1.43kPa	14
2023-12-16 14:00	21.2	0.418	7.7	1.47kPa	24
2023-12-16 15:00	21.2	0.422	7.8	1.46kPa	14
2023-12-16 16:00	21.2	0.413	7.5	1.48kPa	7
2023-12-16 17:00	21.1	0.414	7.5	1.47kPa	17
2023-12-16 18:00	21	0.411	7.3	1.46kPa	27
2023-12-16 19:00	21	0.416	7.4	1.45kPa	17
2023-12-16 20:00	21	0.409	7.2	1.47kPa	7

2023-12-16 21:00	21.1	0.42	7.7	1.45kPa	14
2023-12-16 22:00	21.2	0.41	7.4	1.49kPa	8
2023-12-16 23:00	21.2	0.422	7.8	1.46kPa	7
2023-12-17 0:00	21.4	0.421	8	1.48kPa	7
2023-12-17 1:00	21.2	0.412	7.5	1.48kPa	19
2023-12-17 2:00	20.7	0.41	7	1.44kPa	12
2023-12-17 3:00	20.5	0.409	6.8	1.43kPa	7
2023-12-17 4:00	20.3	0.407	6.5	1.41kPa	8
2023-12-17 5:00	20.1	0.407	6.3	1.40kPa	7
2023-12-17 6:00	20.1	0.405	6.3	1.40kPa	7
2023-12-17 7:00	19.9	0.404	6	1.38kPa	10
2023-12-17 8:00	19.7	0.403	5.8	1.37kPa	15
2023-12-17 9:00	19.6	0.402	5.7	1.36kPa	7
2023-12-17 10:00	19.6	0.412	6.1	1.34kPa	10
2023-12-17 11:00	19.9	0.413	6.4	1.36kPa	8
2023-12-17 12:00	20.2	0.426	7.1	1.36kPa	10
2023-12-17 13:00	20.6	0.429	7.5	1.39kPa	7
2023-12-17 14:00	20.9	0.417	7.4	1.44kPa	7
2023-12-17 15:00	20.7	0.412	7	1.44kPa	7
2023-12-17 16:00	20.7	0.408	6.9	1.45kPa	8
2023-12-17 17:00	20.6	0.405	6.7	1.44kPa	12
2023-12-17 18:00	20.3	0.406	6.5	1.41kPa	8
2023-12-17 19:00	20.2	0.41	6.5	1.40kPa	7
2023-12-17 20:00	20.2	0.412	6.6	1.39kPa	7
2023-12-17 21:00	20.4	0.413	6.8	1.41kPa	7
2023-12-17 22:00	20.6	0.409	6.8	1.43kPa	10
2023-12-17 23:00	20.9	0.428	7.8	1.41kPa	7
2023-12-18 0:00	21.4	0.433	8.4	1.45kPa	10
2023-12-18 1:00	21.4	0.418	7.9	1.48kPa	7
2023-12-18 2:00	21.2	0.413	7.5	1.48kPa	7
2023-12-18 3:00	21	0.41	7.2	1.47kPa	8
2023-12-18 4:00	20.8	0.41	7.1	1.45kPa	12
2023-12-18 5:00	20.6	0.41	6.9	1.43kPa	7
2023-12-18 6:00	20.4	0.411	6.7	1.41kPa	8
2023-12-18 7:00	20.3	0.411	6.6	1.40kPa	10
2023-12-18 8:00	20.3	0.415	6.8	1.39kPa	10
2023-12-18 9:00	20.7	0.436	7.9	1.38kPa	10
2023-12-18 10:00	21.1	0.441	8.4	1.40kPa	7
2023-12-18 11:00	21.4	0.436	8.5	1.44kPa	7
2023-12-18 12:00	21.6	0.429	8.4	1.47kPa	10
2023-12-18 13:00	21.5	0.419	8	1.49kPa	8
2023-12-18 14:00	21.3	0.414	7.6	1.48kPa	12
2023-12-18 15:00	21.3	0.421	7.9	1.47kPa	8
2023-12-18 16:00	21.5	0.413	7.8	1.51kPa	7
2023-12-18 17:00	21.6	0.412	7.8	1.52kPa	8
2023-12-18 18:00	21.6	0.423	8.2	1.49kPa	12
2023-12-18 19:00	21.6	0.419	8.1	1.50kPa	15
2023-12-18 20:00	21.3	0.409	7.5	1.50kPa	14
2023-12-18 21:00	21	0.407	7.1	1.47kPa	17
2023-12-18 22:00	20.8	0.407	7	1.46kPa	19
2023-12-18 23:00	20.6	0.414	7	1.42kPa	10
2023-12-19 0:00	20.8	0.417	7.3	1.43kPa	8
2023-12-19 1:00	20.9	0.41	7.1	1.46kPa	14
2023-12-19 2:00	20.9	0.408	7.1	1.46kPa	21
2023-12-19 3:00	20.9	0.407	7	1.47kPa	21
2023-12-19 4:00	20.8	0.405	6.9	1.46kPa	12
2023-12-19 5:00	20.8	0.405	6.9	1.46kPa	14
2023-12-19 6:00	20.8	0.405	6.9	1.46kPa	7
2023-12-19 7:00	20.7	0.405	6.8	1.45kPa	8
2023-12-19 8:00	20.7	0.405	6.8	1.45kPa	8
2023-12-19 9:00	20.9	0.429	7.8	1.41kPa	7
2023-12-19 10:00	21.4	0.432	8.4	1.45kPa	7
2023-12-19 13:00	20.1	0.427	7	1.35kPa	7
2023-12-19 14:00	20.1	0.426	7	1.35kPa	10
2023-12-19 15:00	20.1	0.425	7	1.35kPa	7
2023-12-19 16:00	20	0.426	6.9	1.34kPa	7

2023-12-19 17:00	20	0.431	7.1	1.33kPa	12
2023-12-19 17:50	20.2	0.446	7.7	1.31kPa	10

Appendix 2

This table is from the report Cross-Canada Survey of Radon Concentrations in Homes, a two-year study conducted by Health Canada's National Radon Program in 2012.

Source: Canada, H. (2024, January 3). *Government of Canada*. Canada.ca. https://www.canada.ca/en/health-canada/services/environmental-workplace-health/reports-publications/radon-what-you-need-to-know.html

Province or Territory	Health Region	Health Region Name	Number of Survey Participants	% Below 200 Bq/m^3	% 200 to 600 Bq/m^3	% Above 600 Bq/m^3	% Above 200 Bq/m^3
BC	5922	Fraser North Health Service Delivery Area	109	100.0	0.0	0.0	0.0
BC	5923	Fraser South Health Service Delivery Area	69	100.0	0.0	0.0	0.0
BC	5931	Richmond Health Service Delivery Area	54	100.0	0.0	0.0	0.0
BC	5932	Vancouver Health Service Delivery Area	83	98.8	1.2	0.0	1.2
BC	5933	North Shore/Coast Garibaldi Health Service Delivery Area	81	97.5	2.5	0.0	2.5
BC	5941	South Vancouver Island Health Service Delivery Area	55	98.2	1.8	0.0	1.8
BC	5942	Central Vancouver Island Health Service Delivery Area	109	99.1	0.9	0.0	0.9
BC	5943	North Vancouver Island Health Service Delivery Area	106	99.1	0.9	0.0	0.9
BC	5951	Northwest Health Service Delivery Area	211	94.8	3.8	1.4	5.2
BC	5952	Northern Interior Health Service Delivery Area	208	88.0	10.1	1.9	12.0
BC	5953	Northeast Health Service Delivery Area	200	90.0	9.5	0.5	10.0
YT	6001	Yukon	225	80.4	13.8	5.8	19.6
NT	6101	Northwest Territories	185	94.6	4.9	0.5	5.4
NU	6201	Nunavut	78	100.0	0.0	0.0	0.0

Appendix 3

TIMES COLONIST

JOIN OUR NEWSLETTER

Editorial: Beware the danger of radon gas in homes

The Times Colonist
Nov 1, 2024 12:46 AM
Updated Nov 1, 2024 1:26 AM

Dr. Aaron Goodarzi, right, scientific director of the Evict Radon National Study, and homeowner Henk de Haan stand beside a water well on de Haan's property near Okotoks, Alta., in February. JEFF MCINTOSH, THE CANADIAN PRESS

Listen to this article
00:04:10

A new report out of the University of Calgary shows an alarming increase in the presence of radon gas in homes across Canada.

In 2012, about seven per cent of homes were found to have dangerous quantities of the gas.

Now that figure is 17.8 per cent, meaning that an estimated 10 million Canadians are living in homes with dangerous amounts of radon.

This is of concern because radon exposure is the second leading cause of lung cancer, after cigarette smoking. Around 21,000 Canadians die of lung cancer each year, and perhaps as many as a sixth of those deaths are due to radon exposure.

Radon is formed when the radioactive element radium decays, and being seven times heavier than air, is usually found in basements.

It is colourless, odourless and deadly. When breathed in, it decays into radioactive lead that has a half-life of 22 years — much longer than radon itself. That means it remains in the lungs long enough to cause cancer.

The gas is measured in Becquerels per square metre (Bq/m3), with 200 units of Bq/m3 being the upper safe limit.

Quantities vary widely across the country. The highest levels are found in the B.C. Interior, Atlantic Canada and Yukon, where one in three homes have radon levels at or above the safe level.

By comparison, in the Pacific Coastal region as a whole, only one in 75 homes have that level.

In Victoria, homes average around 22 Bq/m3, with only one in 200 at or exceeding the safe limit. In Vancouver, the average radon count per home is 18 Bq/m3, and only one in 113 exceeds the safe limit.

The easiest way to measure the amount of radon in your home is through the Evict Radon agency, a national research organization that carries out periodic home-based tests. It can be found at evictradon.org.

Test kits can be ordered at a cost of $54. They arrive by mail, and are about the size of a hockey puck.

The kit must be left in the basement, or lowest floor, for three months.

It is then mailed back to the agency with a prepaid return envelope, and a reading is provided within six to eight weeks.